Biogeosciences Discuss., doi:10.5194/bg-2017-107, 2017
Manuscript under review for journal Biogeosciences
Discussion started: 30 March 2017

1. Title page:

Complex controls on nitrous oxide flux across a long elevation gradient in the tropical Peruvian Andes

Torsten Diem[1,2], Nicholas J. Morley[1], Adan Julian Ccahuana[3], Lidia Priscila Huaraca Quispe[3], Elizabeth M. Baggs[4], Patrick Meir[5, 6], Mark I.A. Richards[1], Pete Smith[1], and Yit Arn Teh[1,2]*

[1] School of Biological Sciences, University of Aberdeen, UK
[2] Formerly at the School of Geography and Geosciences, University of St Andrews, UK
[3] Universidad Nacional de San Antonio Abad del Cusco, Peru
[4] The Royal (Dick) School of Veterinary Studies, University of Edinburgh
[5] School of GeoSciences, University of Edinburgh, UK
[6] Research School of Biology, Australian National University, Canberra, Australia

* Corresponding author; yateh@abdn.ac.uk

Biogeosciences Discuss., doi:10.5194/bg-2017-107, 2017
Manuscript under review for journal Biogeosciences
Discussion started: 30 March 2017

2. Abstract

Current bottom-up process models suggest that montane tropical ecosystems are weak atmospheric sources of N_2O, although recent empirical studies from the southern Peruvian Andes have challenged this idea. Here we report N_2O flux from combined field and laboratory experiments that investigated the process-based controls on N_2O flux from montane ecosystems across a long elevation gradient (600-3700 m a.s.l.) in the southern Peruvian Andes. Nitrous oxide flux and environmental variables were quantified in four major habitat types (premontane forest, lower montane forest, upper montane forest and montane grassland) at monthly intervals over a 30-month period from January 2011 to June 2013. The role of soil moisture content in regulating N_2O flux was investigated through a manipulative, laboratory-based ^{15}N-tracer experiment. The role of substrate availability (labile organic matter, NO_3^-) in regulating N_2O flux was examined through a field-based litter-fall manipulation experiment and a laboratory-based $^{15}N\text{-}NO_3^-$ addition study. Ecosystems in this region were net atmospheric sources of N_2O, emitting 0.27 ± 0.07 mg $N\text{-}N_2O$ m^{-2} d^{-1}. Nitrous oxide flux was inversely related to elevation; N_2O flux was greatest in premontane forest (0.75 ± 0.18 mg $N\text{-}N_2O$ m^{-2} d^{-1}), followed by lower montane forest (0.46 ± 0.24 mg $N\text{-}N_2O$ m^{-2} d^{-1}), montane grasslands (0.07 ± 0.08 mg $N\text{-}N_2O$ m^{-2} d^{-1}), and upper montane forest (0.04 ± 0.07 mg $N\text{-}N_2O$ m^{-2} d^{-1}). Nitrous oxide flux showed weak seasonal variation across the region; only lower montane forest showed significantly higher N_2O flux during the dry season compared to wet season. Manipulation of soil moisture content in the laboratory indicated that N_2O flux was significantly influenced by changes in water-filled pore space (WFPS). The relationship between N_2O flux and WFPS was bimodal and non-linear, diverging from theoretical predictions of how WFPS relates to N_2O flux. Nitrous oxide flux was greatest at 90 and 50 % WFPS, and lowest at 70 and 30 % WFPS. This bimodal distribution of N_2O flux suggests a complex relationship between WFPS, environmental variables, and nitrate-reducing processes. Changes in labile organic matter inputs, through the manipulation of leaf litter-fall, did not alter N_2O flux, suggesting that litter inputs have a negligible impact on N_2O flux. Nitrate addition experiments demonstrated that variations in NO_3^- availability constrained N_2O flux. Habitat – a proxy for NO_3^- availability under field conditions – was the best predictor for N_2O flux, with N-rich habitats (premontane forest, lower montane forest) showing significantly higher N_2O flux than N-poor habitats (upper montane forest, montane grassland). Nitrous oxide flux did not respond to short-term changes in NO_3^- concentration.

3. Introduction

The tropics are the largest source of atmospheric nitrous oxide (N_2O), accounting for at least half of all global emissions (Hirsch et al., 2006;Huang et al., 2008;Kort et al., 2011;Nevison et al., 2007;Saikawa et al., 2014). The bulk of tropical N_2O emissions come from terrestrial sources, with the largest emissions arising from agricultural land and unmanaged lowland tropical forests (Hirsch et al., 2006;Huang et al., 2008;Kort et al., 2011;Nevison et al., 2007;Saikawa et al., 2014). However, while we have a relatively robust understanding of the global atmospheric budget as a whole (Hirsch et al., 2006;Huang et al., 2008;Saikawa et al., 2014), our knowledge of regional atmospheric budgets, particularly at the sub-continental scale, is much more limited, due to the constraints imposed by the spatial distribution of existing atmospheric sampling networks and ground-based, ecosystem-scale sampling efforts (Kort et al., 2011;Nevison et al., 2004;Nevison et al., 2007;Saikawa et al., 2014).

In order to predict and model N_2O flux at these smaller (sub-continental) spatial scales, bottom-up emissions inventories or process-based models are often used, with emissions estimates constrained by empirical measurements (Werner et al., 2007;Li et al., 2000;Potter et al., 1996;Saikawa et al., 2013). However, these models are only as reliable as the data used to parameterize them; as a consequence, ecosystems that are under-represented in the empirical literature or which are poorly understood may be modelled less accurately, with knock-on effects for larger-scale emissions estimates (Saikawa et al., 2013;Teh et al., 2014;Werner et al., 2007). Nitrous oxide dynamics in montane tropical ecosystems are particularly poorly understood, because past research has concentrated on N_2O flux from lowland *tierra firme* forests (Saikawa et al., 2013;Teh et al., 2014;Werner et al., 2007). Montane ecosystems, however, are important components of many tropical landscapes, and account for a sizeable land area. For example, in continental South America, montane ecosystems (>500 m a.s.l.) cover more than 8 % of the land surface (Eva et al., 2004), and play key roles in regional carbon (C), nitrogen (N), and greenhouse gas (GHG) dynamics (Girardin et al., 2010;Moser et al., 2011;Teh et al., 2014;Wolf et al., 2012;Wolf et al., 2011). Process-based models predict that N_2O flux from these montane environments are lower than those from the lowland tropics (i.e. <1.0 kg N_2O-N ha^{-1} yr^{-1}) (Saikawa et al.,

2013;Werner et al., 2007). However, these models have rarely been tested against empirical data, and several field studies indicate that N_2O flux from montane ecosystems can exceed these prior models' estimates (Corre et al., 2010;Teh et al., 2014;Veldkamp et al., 2008). In some instances, N_2O flux from montane ecosystems can in fact approach emissions from lowland forests, begging the question as to whether or not existing models do, in fact, accurately represent flux from these high elevation ecosystems (Corre et al., 2010;Teh et al., 2014;Veldkamp et al., 2008).

In order to improve our wider understanding of the dynamics and biogeochemistry of N_2O in montane tropical forests, we conducted a combination of field- and laboratory-based studies to investigate the environmental controls on denitrification and N_2O flux across a long elevation gradient (600-3700 m a.s.l.) in the tropical Peruvian Andes. Prior work from this region indicated that montane ecosystems in this region were stronger sources of N_2O than predicted by prior bottom-up process models (Teh et al., 2014). In particular, lower elevation premontane and lower montane forests, which are areally-dominant in this region, showed emission rates that are on par with lowland tropical forests, suggesting that these ecosystems could be important contributors to regional atmospheric budgets (Teh et al., 2014). Nitrous oxide flux appeared to be derived from (i.e. denitrification, dissimilatory to ammonium), and were linked to seasonal variations in climate, with N_2O emissions increasing during the dry season compared to the wet season (Teh et al., 2014). However, contrary to theoretical expectations (Davidson, 1991;Firestone and Davidson, 1989;Groffman et al., 2009), N_2O flux was not directly influenced by soil moisture content in our field dataset (Teh et al., 2014), raising important questions about the role of soil moisture as a proximate driver of N_2O flux. Nitrous oxide flux appeared to be more strongly constrained by the availability of substrates for , particularly the availability of nitrate (NO_3^-) (Teh et al., 2014).

In this study, we extended our time series to multi-annual time scales, in order to better understand the role of longer-term climatic variability in modulating N_2O flux, and to investigate the mechanistic controls on N_2O flux (e.g. substrate availability, soil moisture) in greater detail. We also conducted a series of complementary field and laboratory experiments to evaluate key process-based controls on N_2O flux, such as soil moisture

content, labile carbon availability, and NO_3^- availability. The overarching goals of this research were to: investigate how climate and environmental variables regulate N_2O flux over multi-annual time scale; clarify the role of soil moisture as a proximate or distal driver of N_2O flux; and evaluate the role of key substrates, such as labile organic matter and NO_3^-, for driving N_2O flux. Specifically, we hypothesized that:

H1. *Seasonal variations in key environmental variables (e.g. soil moisture content, NO_3^-) drive patterns in N_2O flux on multi-annual time scales*

H2. *N_2O flux increases proportionately with soil moisture content*

H3. *N_2O flux increases proportionately with the availability of substrates for nitrate reduction (i.e. labile organic matter, NO_3^-)*

To address these hypotheses, we conducted a combined field and laboratory study, including monthly field flux measurements collected across a range of elevations and habitats over a 30-month period; a laboratory-based soil moisture manipulation experiment; a field-based litter-fall manipulation study; and a laboratory-based NO_3^- addition study.

4. Materials and methods

4.1 Study site

Measurements were conducted on the eastern slope of the Andes in the Kosñipata Valley, Manu National Park, Peru (Figure 1) (Malhi et al., 2010). This 3.02 x 10^6 ha (30,200 km^2) region has been the subject of intensive ecological, biogeochemical and climatological studies since 2003 by the Andes Biodiversity and Ecosystem Research Group (or, ABERG; http://www.andesconservation.org), and contains a series of long-term permanent plots across a 200-3700 m above sea level (m a.s.l) elevation gradient that stretches from the western Amazon to the Andes (Malhi et al., 2010). This part of the Andes experiences pronounced seasonality in rainfall but not in air temperature; the dry season extends from May to September and the wet season from October to April (Girardin et al., 2010). Thirteen sampling plots (approximately 20 x 20 m each) were established at four different habitats across a gradient spanning 600-3700 m a.s.l., including premontane forest (600 – 1200 m a.s.l.; n = 3 plots), lower montane forest (1200 – 2200 m a.s.l.; n = 3 plots), upper montane forest (2200 – 3200 m a.s.l.; n = 3 plots), and montane grasslands (3200 – 3700 m a.s.l.; n = 4 plots; colloquially referred to as "puna") (Figure 1). In premontane forest, sampling plots

were established in Hacienda Villa Carmen, a 3,065 ha biological reserve operated by the Amazon Conservation Association (ACA), containing a mixture of old-growth forest, secondary forest and agricultural plots (Teh et al., 2014). Sampling for soil gas flux was concentrated in the old-growth portions of the reserve. For lower montane and upper montane forests, sampling plots were established adjacent to or within existing 1 ha permanent sampling plots established by ABERG (Teh et al., 2014). Sampling plots were also established in montane grasslands (Teh et al., 2014). To capture a representative range of environmental conditions, mesotope-scale (100 m-1 km scale landforms) topographic features were sampled (Belyea and Baird, 2006). Mesotopic features include ridges, slopes, flats and a high elevation basin. The latter two landforms include wet, grassy lawns with no discernible grade, and a peat-filled depression, respectively. Summary site descriptions are provided in Table 1. Data on soil properties were collected as part of this study, while mean annual precipitation is from earlier research by ABERG (Girardin et al., 2010).

4.2 Soil-atmosphere exchange

Field sampling was performed over a 30-month period from January 2011 to June 2013 for all habitats except for premontane forest. Because of circumstances outside our control, only 24-months of data were collected for premontane forest, with sampling commencing in July 2011. Soil-atmosphere flux was collected monthly, except where flooding or landslides prevented safe access by investigators to the study sites. Gas exchange rates were determined with five replicate gas flux chambers deployed in each of the thirteen plots (n = 65 flux observations per month). All representative landforms were sampled in each habitat (Table 1).

Soil-atmosphere flux of CH_4, N_2O and CO_2 were determined using a static flux chamber approach (Livingston and Hutchinson, 1995), although only N_2O flux are reported here. Methane and CO_2 flux are discussed in detail in another publication (Jones et al., 2016). Static flux chamber measurements were made by enclosing a 0.03 m^2 area with cylindrical, opaque (i.e. dark), two-component (i.e. base and lid) vented chambers. Chamber bases were permanently installed to a depth of approximately 5 cm and inserted >1 month prior to the commencement of sampling, in order to minimise potential artefacts from root mortality following base emplacement (Varner et al., 2003). Chamber lids were fitted with small

computer case fans to promote even mixing in the chamber headspace (Pumpanen et al., 2004). Headspace samples were collected from each flux chamber over a 30-minute enclosure period, with samples collected at 4 discrete intervals using a gastight syringe. Gas samples were stored in evacuated Exetainers® (Labco Ltd., Lampeter, UK), shipped to the UK by courier, and subsequently analysed for CH_4, N_2O and CO_2 concentrations with a Thermo TRACE GC Ultra (Thermo Fisher Scientific Inc., Waltham, Massachusetts, USA) at the University of St Andrews. Chromatographic separation was achieved using a Porapak-Q column, and analyte concentrations quantified using a flame ionization detector (FID) for CH_4, electron capture detector (ECD) for N_2O, and methanizer-FID for CO_2. Instrumental precision was determined by repeated analysis of standards and was better than 5 % for all detectors. Gas flux rates were determined using the R HMR package to plot best-fit lines to the data for headspace concentration against time for individual flux chambers (Pedersen et al., 2010;R Core Team, 2012). Gas mixing ratios (ppm) were converted to areal flux by using the Ideal Gas Law to solve for the quantity of gas in the headspace (on a mole or mass basis), normalized by the surface area of each static flux chamber (Livingston and Hutchinson, 1995).

4.3 Environmental variables

To investigate the effects of environmental variables on trace gas dynamics, we determined soil moisture, soil oxygen content in the 0-10 cm depth, soil temperature, and air temperature at the time of flux sampling. Volumetric soil moisture content was determined using portable soil moisture probes (ML2x ThetaProbe, Delta-T Device Ltd., Cambridge, UK) inserted into the substrate immediately adjacent to each flux chamber (<5 cm from each chamber base; depth of 0-10 cm). Soil moisture content is reported here as water-filled pore space (WFPS), and is calculated using the measurements of volumetric water content and bulk density (Breuer et al., 2000). Soil O_2 concentration was determined using the approach described by Teh et al. (2014). Soil temperature (0-10 cm depth), chamber temperature and air temperature was determined using type K thermocouples (Omega Engineering Ltd., Manchester, UK). Data on aboveground litter-fall, meteorological variables (i.e. photosynthetically active radiation, air temperature, relative humidity, rainfall, wind speed, wind direction), continuous plot-level soil moisture (10 and 30 cm depths) and soil

temperature (0, 10, 20 and 30 cm depths) measurements were also collected, but are not reported in this publication.

Resin-extractable inorganic N flux (i.e. ammonium, NH_4^+; nitrate, NO_3^-) were quantified in all plots using a resin bag approach (Templer et al., 2005;Subler et al., 1995). From August 2011 onwards, ion exchange resin bags (n = 15 resin bags per elevation) were deployed at the bottom of the plant rooting zone (i.e. 0-10 cm depth in premontane forest, lower montane forest and montane grasslands; 0-15 cm in upper montane forest), following established protocols (Templer et al., 2005;Subler et al., 1995). Samples were collected at monthly intervals (where possible) for determination of monthly, time-averaged NH_4^+ and NO_3^- flux (Subler et al., 1995). For some plots, this sampling frequency was periodically disrupted due to natural hazards (i.e. landslides, river flooding) preventing safe access to the study sites. Resin bags were shipped to the University of Aberdeen after collection from the field, inorganic N was extracted using 2 M KCl and concentrations determined colourimetrically using a Burkard SFA2 continuous-flow analyser (Burkard Scientific Ltd., Uxbridge, UK) (Templer et al., 2005;Subler et al., 1995).

4.4 Water-filled pore space manipulation study

We investigated the effects of WFPS on N_2O flux derived from nitrate reduction or nitrification rates using a ^{15}N tracer experiment. Soil cores for all habitats were collected from the 0-10 cm depth, distributed into glass jars and adjusted to 10% below the target WFPS values of 30%, 50%, 70% and 90% (n = 5 for each ^{15}N addition and 3 controls for each WFPS for a total of n = 212; see Table 2). Additional de-ionized water was added gravimetrically to raise WFPS to target levels. The exception to this was for the upper montane forest, where samples were collected from the 0-10 cm depth of the mineral soil, but not from the organic layer. Two different types of ^{15}N-tracers were applied to the soils in order to determine the proportion of N_2O derived from nitrate reduction and nitrification (Bateman and Baggs, 2005). $^{14}N\text{-}NH_4{}^{15}N\text{-}NO_3$ was used to quantify the amount of N_2O produced by nitrate reduction, while $^{15}N\text{-}NH_4{}^{15}N\text{-}NO_3$ was used to quantify the amount of N_2O produced from both nitrate reduction and nitrification. The difference between the two was used to calculate the amount of N_2O derived from nitrification alone. After application of the tracers, the jars were sealed, and gas samples taken at 0, 6, 12, 24, 36 and 48 hours to

determine rates of gas flux. Nitrous oxide yield was calculated as the ratio of $^{15}N\text{-}N_2O$ flux : $^{15}N\text{-}N_2O$ flux + $^{15}N\text{-}N_2$ flux. Soils were sampled at the end of the experiment for NO_3^- concentration, NH_4^+concentraion, and total C and N content.

Soil gas concentrations (N_2O, CO_2 and CH_4) were measured on a GC as described in section 4.2, while $^{15}N\text{-}N_2$ and $^{15}N\text{-}N_2O$ were measured on a SerCon 20:20 isotope ratio mass spectrometer equipped with an ANCA TGII pre-concentration module (SerCon Ltd., UK). The coefficient of variation (CV; an index of instrumental precision) for repeated analysis of gas concentration and isotope standards was <5 %. $^{15}N\text{-}N_2O$ and $^{15}N\text{-}N_2$ fluxes were calculated from the ^{15}N atom percent excess of the samples compared to the controls using the HMR package (Pedersen et al., 2010). Nitrous oxide yield was calculated as the ratio of $^{15}N\text{-}N_2O$ flux : $^{15}N\text{-}N_2O$ flux + $^{15}N\text{-}N_2$ flux.

4.5 Litter-fall manipulation experiments

We conducted a field-based litter-fall manipulation experiment to test for the effects of variations in labile organic matter availability on trace gas flux. This study took place over a 14-month period (April 2012 to June 2013), and consisted of 4 experimental treatments (control, +50 % litter addition, +100 % litter addition, litter removal) implemented across 3 habitats (premontane forest, lower montane forest, upper montane forest), with 6 replicate plots per treatment per habitat (each treatment plot was 0.5 x 0.5 m in size; n = 24 observations per habitat; n = 72 observations per sampling increment). Leaf litter addition rates for the +50 % and +100 % litter addition treatments were determined based on prior research from this study site, and fell within the natural range of variability observed across this elevational gradient (Girardin et al., 2010).

Litter-fall for the litter addition treatments was collected monthly in litter baskets (n = 3 litter baskets per treatment plot for a total of n = 18 per habitat). These data were also used to determine the background rates of leaf litter-fall among habitats. For the control, litter inputs simply reflected natural background litter-fall rates. For the +50 % and +100 % litter addition treatments, background litter inputs were supplemented with additional litter taken from the litter baskets. Briefly, wet litter was weighed in the field using portable scale, gently mixed (homogenized), and then re-distributed to the +50 % and +100 % litter addition

plots in amounts proportional to the average amount of wet litter that fell into the litter baskets over the course of the month. As a consequence, the amount of litter added in the two litter addition treatments was not fixed but varied according to the natural background rate of litter-fall. For the litter removal treatment, leaf litter was removed from the forest floor at the start of the experiment, and 3mm nylon mesh was placed over the surface of the treatment plot to prevent further litter ingress to the soil surface. Any debris accumulating on the mesh was removed at monthly intervals.

Trace gas flux and environmental variables were determined at 7 time points over the course of the 14-month experiment using the methods described in section 4.2. In addition, soil moisture (WFPS from the 0-10 cm depth), soil temperature (0-10 cm depth), air temperature, soil gas concentrations (O_2, CH_4, N_2O, CO_2) from the 0-10 cm and 20-30 cm depths, litter C, and litter N were determined concomitantly. Litter C and N content was determined on a Carlo-Erba NA 2500 elemental analyser (CE Instruments Ltd, Wigan, UK) at the University of Aberdeen.

4.6 Nitrate addition experiment

To quantify the effect of NO_3^- availability on N_2O flux, we conducted a $^{15}N\text{-}NO_3^-$ addition experiment. Background concentrations of NO_3^- were determined prior to the start of experiment using soil subsamples, after which the soils from each habitat were divided into three treatment groups, and supplemented with surplus NO_3^- which raised these background levels by +50 %, +100 %, and +150 % (Table 2). The NO_3^- added to the soil in each of the treatments was enriched with ^{15}N in order to trace the conversion of nitrate to gaseous N products ($^{15}N\text{-}N_2O$, $^{15}N\text{-}N_2$) (Baggs, 2003;Bateman and Baggs, 2005).

Soil cores were sampled from 0-10 cm for each habitat (n = 6 soil cores per habitat), with the exception for upper montane forest, where two separate sets of cores were collected, one from the organic layer (O horizon; n = 6) and the other from the mineral layer (A horizon; n = 6). Soil samples were then shipped to the University of Aberdeen. Five of these soil cores were split into four equal parts (3 treatment cores and one control core) and distributed into 1 L screw top jars (Kilner, UK). A small soil subsample from each core was used to determine WFPS, background NO_3^- content (extracted in 100ml 1M KCl for a 10g soil sample prior to the

start of the experiment), as well as total C and N content. If necessary, the cores were gravimetrically amended with water until the cores reached 80% WFPS. Soil cores were kept under constant conditions for 3 days before the start of the experiment to minimise the effects of changing water content on soil processes.

At the start of the experiment, dissolved ^{15}N-labelled KNO_3 (30 atom %) was added according to the measured NO_3^- concentrations of each core to reach the required NO_3^- concentration for each treatment (Table 2). Initial NO_3^- concentration (prior to ^{15}N addition) averaged (± standard error) 157 ± 12 µg N g soil^{-1} for pre-montane forest, 140 ± 12 µg N g soil^{-1} for lower montane forest, 19 ± 7 µg N g soil^{-1} for upper montane forest organic layer soil, 18 ± 5 µg N g soil^{-1} for upper montane forest mineral layer soil, and 6 ± 2 µg N g soil^{-1} for montane grassland soil (Table 2). The jars were then sealed with lids fitted with a two-way stopcock to allow for gas sampling. Gas samples were taken with gas tight syringes, and stored in pre-evacuated containers for determination of ^{15}N-N_2, ^{15}N-N_2O, N_2O, CO_2 and CH_4 content. Isotope samples (150 ml) were stored in 100 mL serum bottles and gas concentration samples (20 ml) were stored in 12 ml Exetainers® (Labco Ltd., Lampeter, UK). After gas sampling, the stopcock was opened to allow the sampled air from the jar to be replaced by lab air, and lab air was sampled to allow for correction of the gas concentrations in the jars due to dilution. Samples were taken at 0, 6, 12, 24, 36, and 48 hours, after which the jars were opened and soil was sampled for determination of NO_3^-, NH_4^+ and total C and N. Gas flux, isotopic and elemental concentrations were determined according to the methods described previously.

4.7 Statistics

Statistical analyses were performed using JMP IN Version 8 (SAS Institute, Inc., Cary, North Carolina, USA) or R (R Core Team, 2012). Residuals were checked for heteroscedasticity and homogeneity of variances. Where necessary, the data were transformed using a Box-Cox procedure to meet the assumptions of analysis of variance. Analysis of variance (ANOVA) or Generalized Linear Models were used to evaluate the effect of categorical variables (i.e. site, season, topography) on trace gas flux and environmental variables. Analysis of covariance (ANCOVA) was performed on Box-Cox transformed data to investigate the combined effects of categorical variables and environmental factors (e.g. water-filled pore space, soil oxygen

content, air temperature, soil temperature, etc.) on trace gas flux. Non-parametric tests were employed where Box-Cox transformation was unable to normalize the data, homogenize the variances, or where the residuals still showed strong trends even after Box-Cox transformation. Means comparisons were performed using Fisher's Least Significant Difference test (Fisher's LSD). Statistical significance was determined at the $P < 0.05$ level, unless otherwise noted. Values are reported as means and standard errors (± 1 SE). Statistical analyses for the field data were conducted on plot-averaged data to avoid pseudo-replication.

5. Results

5.1 Variations in N_2O flux among habitats and between seasons

The overall mean N_2O flux for the entire dataset was 0.27 ± 0.07 mg N-N_2O m^{-2} d^{-1}, with a range from -8.40 to 75.0 mg N-N_2O m^{-2} d^{-1}. We investigated the effect of habitat, season, and topography on N_2O flux by using a three-way ANOVA on plot-averaged data ($F_{10,307}$ = 3.28, $P < 0.0005$). We found that there was a significant effect of habitat ($P < 0.003$) and an effect of season at the borderline of statistical significance ($P < 0.07$). However, we found no effect of habitat by season or topography on N_2O flux. Habitat accounted for 4.3 % of the variance in the dataset, while season accounted for only 1.0 % of the variance.

Among habitats, the overall trend was towards the highest flux from premontane forest (0.75 ± 0.18 mg N-N_2O m^{-2} d^{-1}), followed by lower montane forest (0.46 ± 0.24 mg N-N_2O m^{-2} d^{-1}), montane grasslands (0.07 ± 0.08 mg N-N_2O m^{-2} d^{-1}), and upper montane forest (0.04 ± 0.07 mg N-N_2O m^{-2} d^{-1}) (Figure 2a). Multiple comparisons tests indicated that only premontane forests showed statistically higher flux than the others (Fisher's LSD, $P < 0.05$); while there were numerical differences in mean flux among the other habitats, large variances meant that they had overlapping ranges of flux (Figure 2a).

The borderline significant effect of season ($P < 0.07$) reflected an overall trend of higher dry season (0.51 ± 0.18 mg N-N_2O m^{-2} d^{-1}) compared to wet season (0.15 ± 0.07 mg N-N_2O m^{-2} d^{-1}) flux (Table 3). However, part of why the effect of season was weak was because only lower montane forest showed significant variability between seasons (Fisher's LSD, $P < 0.05$), while

the other three habitats did not show significant seasonal differences in flux (Fisher's LSD, $P < 0.05$).

Even though the effect of topography alone was not statistically significant within the context of the three-way ANOVA, N_2O flux from flat sites were significantly higher (0.62 ± 0.28 mg N-N_2O m^{-2} d^{-1}) than from the basin site (-0.18 ± 0.16 mg N-N_2O m^{-2} d^{-1}) (Fisher's LSD, $P < 0.05$). However, there was no significant difference between flat sites with slope and ridge sites (0.24 ± 0.09 mg N-N_2O m^{-2} d^{-1} and 0.20 ± 0.08 mg N-N_2O m^{-2} d^{-1}, respectively) (Fisher's LSD, $P > 0.05$).

For each habitat, we also compared individual wet and dry seasons against each other using multiple comparisons tests (e.g. dry season 2012 vs wet season 2012; dry season 2012 vs dry season 2013, etc.) to determine if there was significant year-on-year variation in N_2O flux among multiple seasons. Consistent with our three-way ANOVA results, we found that only lower montane forest showed significant variation among multiple dry and wet seasons, whereas the other habitats showed no significant trends. For lower montane forest, we observed significantly higher dry season flux in 2011 compared to wet and dry seasons in all other years ($P < 0.05$; Figure 3b).

5.2 Variations in environmental conditions among habitats and between seasons

We investigated the effect of habitat, season, and topography on environmental variables by using a three-way ANOVA on plot-averaged data. The environmental variables examined here were water-filled pore space (WFPS) in the 0-10 cm depth, soil temperature, air temperature, gas-phase soil oxygen content in the 0-10 cm depth, and resin-extractable inorganic N flux (NH_4^+, NO_3^-).

Water-filled pore space varied significantly as a function of habitat, season, habitat by season, and topography ($F_{10,304}$ = 637.96, $P < 0.0001$; Table 3, Figure 2b, Figure 3). Habitat accounted for the largest proportion of variance in the model (78.1 % of the total variance), followed by season (0.6 %), habitat by season interaction (0.6 %), and topography (0.4 %). Each habitat differed significantly from the others (Fisher's LSD, $P <0.05$), with the highest WFPS observed in montane grassland (88.4 ± 0.3 %), followed by premontane forest (51.6 ±

1.3 %), lower montane forest (39.0 ± 0.9 %), and upper montane forest (35.0 ± 1.5 %) (Figure 2b). WFPS varied significantly between seasons (t-Test, $P < 0.05$), with a mean dry season value of 52.1 ± 2.4 % compared to a mean wet season value of 59.5 ± 1.6 % (Table 3). The significant habitat by season interaction is due to the fact that some habitats showed seasonal trends in WFPS whereas others did not. Whereas lower montane and upper montane forests all showed a significant reduction in WFPS during the dry season, premontane forest and montane grasslands showed no seasonal differences in WFPS (Table 3, Figure 3). For topography, the main effect was that the basin landform had significantly higher WFPS than the other landforms. The basin landform showed a mean WFPS of 89.3 ± 0.1 % whereas WFPS in other landforms ranged from 51.7 ± 2.2 to 57.7 ± 2.7 %.

Soil oxygen in the 0-10 cm depth varied as a function of habitat, habitat by season, and topography ($F_{10,242} = 27.70$, $P < 0.0001$; Table 3). The effect of season was significant at the $P < 0.06$ level. Habitat accounted for the largest proportion of variance in the model (66.9 % of the total variance), followed by topography (8.4 %), habitat by season (3.5 %), and season alone (0.7 %). For habitat, multiple comparisons tests indicated that montane grasslands showed significantly lower soil O_2 content than the other habitats (13.5 ± 0.6 %), whereas the other habitats showed statistically similar soil O_2 values to each other (18.6 ± 0.2 to 19.5 ± 0.1 %; Fisher's LSD, $P < 0.05$). For topography, multiple comparisons tests indicated that the basin landform showed statistically lower soil O_2 content than the other landforms (7.4 ± 2.3 %), whereas the other topographic features showed statistically similar values, ranging from 16.9 ± 0.6 to 18.2 ± 0.2 % (Fisher's LSD, $P < 0.05$). The significant habitat by season interaction was due to the fact that only montane grassland showed a significant difference in O_2 content between wet and dry season, whereas other habitats showed similar soil O_2 values (Table 3). For season alone, wet season soil O_2 content (16.8 ± 0.4 %) was slightly lower than dry season values (17.8 ± 0.3 %) (t-Test, $P < 0.03$); however, given the significant habitat by season interaction described previously, this weak seasonal trend in the pooled dataset was likely driven by the seasonal pattern in montane grassland.

For soil temperature, the effects of habitat, season, habitat by season, and topography were all significant ($F_{10,292} = 790.7$, $P < 0.0001$). Habitat accounted for the largest proportion of variance in the model (85.5 % of the total variance), followed by season (1.4%), habitat by

season interaction (0.5 %), and topography (0.3 %). Each habitat differed significantly from the others (Fisher's LSD, P <0.05), with the highest soil temperature observed for premontane forest (20.5 ± 0.1 °C), followed by lower montane forest (17.8 ± 0.1 °C), upper montane forest (11.5 ± 0.1 °C), and montane grasslands (10.6 ± 0.2 °C). Soil temperature varied significantly between season (t-Test, $P < 0.05$), with a mean dry season value of 13.9 ± 0.4 °C compared to a mean wet season value of 15.1 ± 0.3 °C. The significant habitat by season interaction is due to the fact that some habitats showed more pronounced seasonal trends in soil temperature than others, although the overall pattern of cooler dry season compared to wet season soil temperatures holds across all habitats (Table 3). For topography, the flat landforms showed significantly higher soil temperatures than the others (16.0 ± 0.5 °C), the basin landform showed significantly lower values (10.8 ± 0.4 °C), whereas ridge and slope landforms showed similar values to each other (14.3 ± 0.4 °C and 14.7 ± 0.4 °C, respectively) (Fisher's LSD, $P < 0.05$).

For air temperature, only the effect of habitat was significant ($F_{10,292}$ = 103.2, $P < 0.0001$; Table 3). A multiple comparisons test indicated that each habitat showed significantly different temperatures compared to the others (Fisher's LSD, $P < 0.05$). Premontane forest showed the highest air temperatures (21.0 ± 0.3 °C), followed by lower montane forest (18.7 ± 0.2 °C), upper montane forest (12.7 ± 0.2 °C), and montane grassland (11.7 ± 0.3 °C). Other variables did not significantly affect air temperature.

For resin-extractable NH_4^+ flux, the three-way ANOVA model was not statistically significant ($F_{10,164}$ = 1.3, $P > 0.2$; Table 3). However, even though the three-way ANOVA as a whole was not statistically significant, the overall trend was towards significantly lower NH_4^+ flux in the dry season (9.6 ± 0.7 µg N-NH_4 g resin^{-1} d^{-1}) compared to the wet season (22.3 ± 3.6 µg N-NH_4 g resin^{-1} d^{-1}).

Resin-extractable NO_3^- flux showed different patterns from NH_4^+ flux, with significant effects of habitat, topography, and habitat by season but not of season alone ($F_{10,164}$ = 39.0, $P <$ 0.0001; Figure 2c, Table 3). Habitat accounted for the largest proportion of the variance (61.5 %), followed topography (4.7 %), and habitat by season (1.9 %). Premontane forest showed the highest NO_3^- flux (22.6 ± 2.0 µg N-NO_3 g resin^{-1} d^{-1}), followed by lower montane

forest (10.0 ± 1.2 μg N-NO_3 g $resin^{-1}$ d^{-1}) (Fisher's LSD, $P < 0.05$; Figure 2c). Upper montane forest (1.1 ± 0.2 μg N-NO_3 g $resin^{-1}$ d^{-1}) and montane grassland (1.7 ± 0.3 μg N-NO_3 g $resin^{-1}$ d^{-1}) showed significantly lower NO_3^- flux than the other two habitats (Fisher's LSD, $P < 0.05$; Figure 2c). However, NO_3^- flux in upper montane forest and montane grassland did not differ significantly from each other (Fisher's LSD, $P > 0.05$; Figure 2c). For the effect of topography, multiple comparisons tests indicated that flat landforms (12.1 ± 1.8 μg N-NO_3 g $resin^{-1}$ d^{-1}) and slope landforms (10.2 ± 1.6 μg N-NO_3 g $resin^{-1}$ d^{-1}) differed significantly from ridge landforms (6.6 ± 1.4 μg N-NO_3 g $resin^{-1}$ d^{-1}) (Fisher's LSD, $P < 0.05$). The basin landform (3.8 ± 1.3 μg N-NO_3 g $resin^{-1}$ d^{-1}), despite the lower mean values, showed an overlapping range with the other landforms (Fisher's LSD, $P > 0.05$). The habitat by season interaction is due to the fact that upper montane forest shows a significant seasonal fluctuation in resin-extractable NO_3^- (Fisher's LSD, $P < 0.05$), whereas the other habitats show no significant seasonal trend (Fisher's LSD, $P > 0.05$).

5.3 Effects of environmental variables on N_2O flux

For the whole dataset, the relationship between N_2O flux and environmental variables was examined using ANCOVA on Box-Cox transformed data with habitat, season, topography, and environmental variables as covariates. Environmental variables included WFPS, oxygen, air temperature, soil temperature, and resin-extractable inorganic N flux (NH_4^+ and NO_3^-). The ANCOVA model as a whole was not statistically significant ($P > 0.4$). However, we found that individual factors were weakly but significantly correlated with N_2O flux for the pooled dataset. These included soil temperature (r^2= 0.04, P <0.0004), air temperature (r^2= 0.04, P <0.0008), and resin-extractable NO_3^- flux (r^2= 0.03, P <0.03). Water-filled pore space also showed a very weak negative correlation with N_2O flux at the borderline of statistical significance (r^2= 0.01, P <0.06).

For individual habitats, we explored how variations in environmental conditions influenced N_2O flux using multiple regression, with WFPS, oxygen, soil temperature, air temperature, resin-extractable NH_4^+ flux, and resin-extractable NO_3^- flux as explanatory variables. Only the multiple regression analysis for lower montane forest showed a borderline significant result, though only at the $P < 0.07$ level (r^2 = 0.36). The multiple regression models for all the other habitats were not statistically significant ($P > 0.4$). Lower montane forest was the only

habitat that showed a significant effect of season on N_2O flux (section 5.1), and our multiple regression model corroborated this result by showing that seasonal fluctuations in air temperature, soil temperature, WFPS (Figure 3b), and NH_4^+ all correlated with N_2O flux ($P < 0.05$). Air temperature explained the largest proportion of variance in the data (26.2 %; negative trend), followed by soil temperature (15.5 %; positive trend), WFPS (13.7 %; negative trend), and resin-extractable NH_4^+ flux (11.6 %; negative trend).

5.4 Water-filled pore space manipulation

^{15}N-N_2O and ^{15}N-N_2 fluxes showed a biphasic response (Limmer and Steele, 1982), with significantly different flux rates in the first 24 hours of incubation compared to the later period of incubation (i.e. >24 hours onwards). Flux of ^{15}N-N_2O, and ^{15}N-N_2 were therefore divided into early (≤24 hours) and late (>24 hours) phase flux.

5.4.1 Role of nitrate reduction in N_2O production

For both the ^{15}N-N_2O and $^{15}N^{-}N_2$ flux data, we conducted an initial analysis using a full factorial ANOVA on Box-Cox transformed data with habitat, moisture level, form of ^{15}N-label added (i.e. $^{15}NH_4{}^{15}NO_3$ or $^{14}NH_4{}^{15}NO_3$), incubation phase, and all their interaction terms as independent variables. Importantly, we found that the form of ^{15}N-label added (i.e. ^{15}N-$NH_4{}^{15}N$-NO_3 or ^{14}N-$NH_4{}^{15}N$-NO_3) did not significantly influence ^{15}N-N_2O or ^{15}N-N_2 flux, because production of either gas from ^{15}N-$NH_4{}^{15}N$-NO_3 addition was modest to negligible (Supplementary Online Materials Figure S1). This indicates that that nitrate reduction was the dominant source of N_2O among these habitats. Thus, in order to simplify our statistical analyses, all subsequent analyses were performed using only habitat, moisture level, incubation phase, and their interaction terms as independent variables. For these tests, which are described below, the "total" flux of ^{15}N-N_2O or ^{15}N-N_2 represents gas produced by both nitrification and nitrate reduction together.

5.4.2 ^{15}N-N_2O flux

For the total ^{15}N-N_2O flux data, we used a full factorial ANOVA on Box-Cox transformed data with habitat, moisture level, incubation phase, and all their interactions as independent variables. We found that moisture level, habitat by incubation phase, and habitat by moisture by incubation phase significantly affected flux, while all other factors were not

statistically significant (ANOVA, $F_{31, 321}$ = 3.05, P < 0.0001; Figure 4). For the moisture level effect, the highest flux was observed for the 90 % WFPS (42 ± 9 ng N_2O-^{15}N g^{-1} d^{-1}) and 50 % WFPS (29 ± 10 ng N_2O-^{15}N g^{-1} d^{-1}) treatments, and the lowest flux for the 30 % (3 ± 1 ng N_2O-^{15}N g^{-1} d^{-1}) and 70 % (7 ± 2 ng N_2O-^{15}N g^{-1} d^{-1}) treatments (Fisher's LSD, P < 0.05; Figure 4).

The habitat by incubation phase interaction indicated that some habitats showed different flux from each other during different phases of the incubation (Figure 4). For example, premontane and lower montane forest showed no significant difference in flux during different incubation phases (t-Test, P > 0.05 for each habitat), whereas upper montane forest mineral layer soils showed a significant increase from early to late incubation phases (5 ± 2 ng N_2O-^{15}N g^{-1} d^{-1} versus 42 ± 13 ng N_2O-^{15}N g^{-1} d^{-}1; t-Test, P < 0.003). In contrast to the other habitats, montane grasslands showed a significant decrease in flux from early to late incubation phases (60 ± 23 ng N_2O-^{15}N g^{-1} d^{-1} versus 6 ± 9 ng N_2O-^{15}N g^{-1} d^{-1}, respectively; t-Test, P < 0.02).

The habitat by moisture by incubation phase effect indicated that different habitats showed varying responses to moisture depending on the incubation phase (Figure 4). For example, for the premontane and lower montane forest, which showed no effect of incubation phase, flux followed the moisture trend described for the data set as a whole (i.e. highest flux for the 90 % WFPS treatment, lowest flux for the 30 % WFPS treatment, intermediate flux for the 50 & 70 % WFPS treatments). In contrast, for upper montane forest mineral layer soils, the effects of moisture varied with incubation phase. During the early phase, flux was highest in the 50 % WFPS treatment (20 ± 8 ng N_2O-^{15}N g^{-1} d^{-1}), while all other treatments showed lower flux (pooled average of 0.5 ± 0.4 ng N_2O-^{15}N g^{-1} d^{-1}). In the late phase, flux was highest for the 90 % WFPS treatment (145 ± 40 ng N_2O-^{15}N g^{-1} d^{-1}) while the other treatments were lower and not statistically different from each other (pooled average: 13 ± 5 ng N_2O-^{15}N g^{-1} d^{-1})

5.4.3 $^{15}N^{-}N_2$ flux

For the total ^{15}N-N_2 flux data, we used a full factorial ANOVA on Box-Cox transformed data with habitat, moisture level, incubation phase, and all their interactions as independent variables. We found that all of the main factors and their interaction terms were statistically

significant (ANOVA, $F_{31, 317}$ = 14.20, P < 0.0001). For the habitat effect, lower montane forest had the highest flux (694 ± 83 ng N_2-^{15}N g^{-1} d^{-1}), while premontane forest and upper montane forest mineral layer collectively had intermediate flux soil (326 ± 53 and 171 ± 20 ng N_2-^{15}N g^{-1} d^{-1}, respectively) (Fisher's LSD, P < 0.05; Figure 4). Montane grassland soil had the lowest flux (123 ± 23 ng N_2O-^{15}N g^{-1} d^{-1}) (Fisher's LSD, P < 0.05; Figure 4). For the moisture effect, only the 90 % treatment had significantly higher flux than the other treatments (90 % WFPS treatment: 437 ± 77 ng N_2-^{15}N g^{-1} d^{-1}; pooled average for all other treatments: 294 ± 28 ng N_2-^{15}N g^{-1} d^{-1}) (Fisher's LSD, P < 0.05). The effect of incubation phase was only significant at the P < 0.1 level, with greater release of ^{15}N-N_2 during the late compared to the early phase of the incubation (373 ± 44 ng N_2-^{15}N g^{-1} d^{-1} versus 288 ± 37 ng N_2-^{15}N g^{-1} d^{-1}) (t-Test, P < 0.07).

The habitat by moisture level interaction indicates that flux from different habitats showed varying moisture responses (Figure 4). For example, flux from premontane forest and upper montane forest mineral layer soil showed no responses to moisture. In contrast, for lower montane forest, flux was greatest for the 90 % WFPS treatment (1,365 ± 201 ng N_2-^{15}N g^{-1} d^{-1}), lowest for the 70 % WFPS treatment (257 ± 128 ng N_2-^{15}N g^{-1} d^{-1}), and at intermediate levels for the 30 and 50 % WFPS treatments (664 ± 131 and 492 ± 79 ng N_2-^{15}N g^{-1} d^{-1}, respectively) (Fisher's LSD, P < 0.05). The pattern for montane grassland was different again; here, only the 90 % WFPS treatment showed significantly greater flux (171 ± 32 ng N_2-^{15}N g^{-1} d^{-1}) compared to the other treatments (pooled average: 105 ± 29 ng N_2-^{15}N g^{-1} d^{-1}) (Fisher's LSD, P < 0.05).

The habitat by incubation phase interaction indicates that flux for different habitats showed different patterns during early and late incubation phases (Figure 4). For example, premontane forest showed a significant increase for early (169 ± 42 ng N_2-^{15}N g^{-1} d^{-1}) to late (483 ± 91 ng N_2-^{15}N g^{-1} d^{-1}) incubation phases (t-Test, P < 0.01. In contrast, lower montane forest, upper montane forest mineral layer soil, and montane grassland all showed no significant change in flux between incubation phases (t-Test, P > 0.05 for all habitats).

Finally, the habitat by moisture level by incubation phase interaction indicates that moisture responses among habitats were influenced by incubation phase (Figure 4). For example, for

the premontane forest, where an incubation phase effect was found, the response to moisture varied depending on incubation phase. During the early phase of the incubation, flux was lowest from the 70 % WFPS treatment (0 ± 0 ng N_2-^{15}N g^{-1} d^{-1}), while all other moisture treatments showed similar levels of flux (pooled average: 224 ± 52 ng N_2-^{15}N g^{-1} d^{-1}). For the late phase, the highest flux was observed for the 70 % WFPS treatment (1,267 ± 175 ng N_2-^{15}N g^{-1} d^{-1}), followed by the 50 % WFPS treatment (540 ± 99 ng N_2-^{15}N g^{-1} d^{-1}), the 90 % treatment (157 ± 43 ng N_2-^{15}N g^{-1} d^{-1}), and the 30 % WFPS treatment (0 ± 0 ng N_2-^{15}N g^{-1} d^{-1}) (Fisher's LSD, $P < 0.05$). In contrast, for all other habitats, where there was no significant incubation phase effect (i.e. lower montane forest, upper montane forest mineral layer soil, montane grassland), the response to moisture followed the overall pattern described previously.

5.4.4 N_2O Yield

For the N_2O yield, we used a full factorial ANOVA on Box-Cox transformed data with habitat, moisture level, incubation phase, and all their interactions as independent variables. We found that habitat, moisture level, habitat by moisture level, habitat by phase, and habitat by moisture level by phase significantly influenced N_2O yield (ANOVA, $F_{31, 313} = 9.85$, $P < 0.0001$). For the habitat effect, N_2O yield was highest for the montane grassland (0.61 ± 0.06), lowest for lower montane forest (0.19 ± 0.04), while premontane forest and upper montane forest mineral layer soil showed similar intermediate values (0.40 ± 0.05 and 0.42 ± 0.05, respectively) (Fisher's LSD, $P < 0.05$). For the moisture level effect, N_2O yield was highest for the 70 % WFPS treatment (0.51 ± 0.06), while the 30, 50 and 90 % WFPS treatments showed statistically similar values (0.35 ± 0.05, 0.39 ± 0.05, and 0.36 ± 0.05, respectively) (Fisher's LSD, $P < 0.05$).

The interaction terms indicated that different habitats showed varying N_2O yield in response to moisture level and incubation phase. For the habitat by moisture level interaction, some habitats showed no effect of moisture level on N_2O yield (i.e. premontane forest, montane grassland), whereas others showed changes in N_2O yield with moisture level. For example, for the lower montane forest, N_2O yield was greatest for the 70 % WFPS treatment (0.51 ± 0.11), whereas the 30, 50 and 90 WFPS % treatments were statistically undifferentiated from each other (pooled average: 0.09 ± 0.03) (Fisher's LSD, $P < 0.05$). Upper montane forest

mineral layer soil showed the highest N_2O yield for the 90 % treatment (0.72 ± 0.08), lowest yield for the 30 % WFPS treatment (0.20 ± 0.09), and intermediate N_2O yields for the 50 and 70 % WFPS treatments (0.29 ± 0.09 and 0.50 ± 0.11, respectively) (Fisher's LSD, $P < 0.05$). For the habitat by phase interaction, some habitats showed no effect of incubation phase on N_2O yield (i.e. premontane and lower montane forest), whereas some showed an increase in N_2O yield from early to late phase (i.e. upper montane forest mineral layer soil), while still others showed a decrease in N_2O yield from early to late phase (i.e. montane grassland). For the upper montane forest mineral layer soil, N_2O yield shifted from 0.33 ± 0.07 to 0.51 ± 0.07 (t-Test, $P < 0.04$), while for montane grassland N_2O yield changed from 0.70 ± 0.07 to 0.52 ± 0.09 (t-Test, $P < 0.05$).

The habitat by moisture level by incubation phase interaction reflects the fact that the moisture response of different habitats was contingent upon incubation phase. For instance, for upper montane forest mineral layer soil, N_2O yield during the early phase was greatest for the 90 % WFPS treatment (1; i.e. no $^{15}N\text{-}N_2$ flux observed), while the 50 % WFPS treatment showed intermediate N_2O yield (0.33 ± 12), and the 30 and 70 % WFPS treatments collectively showed the lowest N_2O yields (approximately 0 for both; i.e. no $^{15}N\text{-}N_2O$ flux observed) (Fisher's LSD, $P < 0.05$). In contrast, during the late phase, the 70 % WFPS treatment showed the highest N_2O yield (1; i.e. no $^{15}N\text{-}N_2$ flux observed), while the other treatments showed lower N_2O yields that were not significantly different from each other (pooled average: 0.33 ± 0.07) (Fisher's LSD, $P < 0.05$). In contrast, for montane grassland, no effect of moisture was observed during the early phase of the incubation. However, during the late phase, the 50 % WFPS treatment showed the highest N_2O yield (0.89 ± 0.11), while the other treatments showed lower N_2O yields that were not significantly different from each other (pooled average: 0.39 ± 0.10) (Fisher's LSD, $P < 0.05$). For all other habitats with no habitat by phase interaction (i.e. premontane and lower montane forest), the moisture effect follows the general trends described above.

5.5 Litter manipulation experiment

In order to investigate the relationship between leaf litter input rates and N_2O flux, we used a Generalized Linear Model (GLM) and an ANCOVA that included habitat, litter treatment, season, WFPS, litter input rate, litter C input rate, litter N input rate, soil temperature and air

temperature as independent variables. The analysis was also repeated using ANCOVA on Box-Cox transformed data. Both analyses revealed no significant statistical relationship between N_2O flux and any of these environmental variables, with the exception of soil temperature, which showed only a weak positive relationship to N_2O flux when the data was analysed using the GLM ($P < 0.05$). This relationship was not detected using ANCOVA. Bivariate regression of soil temperature against N_2O flux indicated that the relationship was relatively weak, with $r^2 = 0.01$ ($P < 0.05$).

5.6 Nitrate addition experiment

^{15}N-N_2O and ^{15}N-N_2 fluxes showed a biphasic response (Limmer and Steele, 1982), with significantly different flux rates in the first 24 hours of incubation compared to the later period of incubation (i.e. >24 hours onwards). Flux of ^{15}N-N_2O, and ^{15}N-N_2 were therefore divided into early (≤24 hours) and late (>24 hours) phase flux.

5.6.1 ^{15}N-N_2O flux

For the ^{15}N-N_2O flux data, we used a full factorial ANOVA on Box-Cox transformed data with habitat, N addition level, incubation phase, and all their interaction terms as independent variables. Habitat, incubation phase, and a habitat by incubation phase interaction all significantly influenced flux, while N addition level and all other interaction terms were not statistically significant (ANOVA, $F_{29, 149} = 5.66$, $P < 0.0001$; Figure 5). For habitat, upper montane forest organic layer soils showed the highest flux (238 ± 160 ng N_2O-^{15}N g^{-1} d^{-1}) (Fisher's LSD, $P < 0.05$). This was followed by lower montane (179 ± 48 ng N_2O-^{15}N g^{-1} d^{-1}) and premontane (86 ± 16 ng N_2O-^{15}N g^{-1} d^{-1}) forest, which collectively showed intermediate flux (Fisher's LSD, $P < 0.05$). Last, the lowest flux was observed for montane grasslands (11 ± 4 ng N_2O-^{15}N g^{-1} d^{-1}), followed by upper montane forest mineral layer soils (0.06 ± 0.01 ng N_2O-^{15}N g^{-1} d^{-1}) (Fisher's LSD, $P < 0.05$). The high rate of flux attributed to the upper montane forest organic layer soils was due to a strong effect of phase, with significant increase in flux during the late phase of the incubation (Figure 5). For the incubation phase effect, late phase flux was significantly greater than early phase flux (164 ± 66 ng N_2O-^{15}N g^{-1} d^{-1} versus 42 ± 11 ng N_2O-^{15}N g^{-1} d^{-1}; t-Test, $P < 0.05$; Figure 5).

For the habitat by incubation phase interaction, further investigation revealed that this relationship arose from the fact that different habitats varied in their flux during early and late incubation phases (Figure 5). For example, during the early phase, lower montane and premontane forests collectively showed the highest flux (Figure 5; 133 ± 46 and 64 ± 19 ng N_2O-^{15}N g^{-1} d^{-1}, respectively) (Fisher's LSD, $P < 0.05$). Upper montane forest organic layer soils and montane grassland soils collectively showed intermediate rates of flux (Figure 5; 8 ± 2 and 4 ± 1 ng N_2O-^{15}N g^{-1} d^{-1}, respectively), while upper montane forest mineral layer soils showed the lowest flux (Figure 5; 0.04 ± 0.01 ng N_2O-^{15}N g^{-1} d^{-1}) (Fisher's LSD, $P < 0.05$). In contrast, during the late phase, upper montane forest organic layer soils, lower montane forest, and premontane forest now collectively showed the highest flux (469 ± 313 ng N_2O-^{15}N g^{-1} d^{-1}, 224 ± 85 ng N_2O-^{15}N g^{-1} d^{-1}, and 108 ± 25 ng N_2O-^{15}N g^{-1} d^{-1}, respectively). The lowest flux was from montane grasslands (18 ± 7 ng N_2O-^{15}N g^{-1} d^{-1}), followed by upper montane forest mineral layer soils (0.08 ± 0.02 ng N_2O-^{15}N g^{-1} d^{-1}) (Fisher's LSD, $P < 0.05$).

5.6.2 ^{15}N-N_2 flux

For the ^{15}N-N_2 flux data, we used a full factorial ANOVA on Box-Cox transformed data with habitat, N addition level, incubation phase, and all their interaction terms as independent variables. Only habitat significantly influenced flux (Figure 5), while other terms were not significant (ANOVA, $F_{29, 149} = 1.66$, $P < 0.05$). Lower montane and upper montane forest organic layer soils showed the highest flux (472 ± 139 and 576 ± 117 ng N_2-^{15}N g^{-1} d^{-1}, respectively), while all other habitats showed similar flux rates (105 ± 19 ng N_2-^{15}N g^{-1} d^{-1}) (Fisher's LSD, $P < 0.05$; Figure 5).

5.6.3 N_2O Yield

For the N_2O yield, we used a full factorial ANOVA on Box-Cox transformed data with habitat, N addition level, incubation phase (i.e. early versus late), and all their interaction terms as independent variables. We found that none of these factors predicted N_2O yield (ANOVA, $F_{29, 149} = 0.75$, $P > 0.82$). The overall mean N_2O yield for the pooled dataset was 0.53 ± 0.04.

6. Discussion

6.1 Multi-annual trends in N_2O flux among habitats and between seasons

Montane forest and grassland ecosystems in the Kosñipata Valley were net sources of atmospheric N_2O, affirming our prior results (Teh et al., 2014). The flux for this multi-annual dataset were comparable to the preliminary values reported in our earlier publication, with mean flux of 0.27 ± 0.07 mg N-N_2O m^{-2} d^{-1} observed here over a 30 month period, compared with 0.22 ± 0.12 mg N-N_2O m^{-2} d^{-1} recorded over 13 months (Teh et al., 2014). Consistent with our earlier report, flux from our Peruvian transect were greater than those from a comparable study site in Ecuador (Wolf et al., 2011), which we attributed to higher N content in lower elevation soils in Peru (Teh et al., 2014). The elevational trends reported earlier still hold true for this multi-annual dataset (Teh et al., 2014); namely, significantly greater N_2O flux from lower elevation habitats (premontane forest, lower montane forest) compared to higher elevation ones (upper montane forest, montane grasslands) (Figure 2a). More favourable environmental conditions at lower elevations may explain these trends (e.g. higher N availability, warmer temperatures; see below for further details).

Nitrous oxide flux for the Kosñipata Valley varied between seasons, with significantly greater flux during the dry season compared to the wet season (Teh et al., 2014). However, this overall trend was strongly influenced by the behaviour of lower montane forest, which showed pronounced seasonality in N_2O flux, whereas the other habitats showed little or no seasonal differences (Table 3). For premontane forest, upper montane forest, and montane grassland, weak seasonality in N_2O flux may reflect the fact that environmental variables did not vary strongly between seasons (Table 3), challenging our first hypothesis (**H1**). Instead, environmental variables tended to vary more strongly among habitats (section 5.2). Analysis of the environmental data repeatedly demonstrated that habitat accounted for the largest proportion of variance in ANOVA models, with season accounting for a substantially smaller proportion of the variance or none at all. Moreover, in cases where environmental variables differed significantly between seasons, the actual numerical differences were often relatively slight (Table 3). For example, while WFPS varied significantly between seasons, the numerical difference in WFPS between dry season and wet season was 7.4 % WFPS for the pooled data; i.e. 52.1 ± 2.4 versus 59.5 ± 1.6 % WFPS, respectively. Likewise, oxygen in the 0-10 cm soil depth varied by less than 1 %, with a mean dry season value of 17.8 ± 0.3 % compared to a wet season value of 16.8 ± 0.4 %. Soil temperature varied by less than 1.2 °C, with a mean dry season value of 13.9 ± 0.4 °C compared to a wet season value of 15.1 ± 0.3

°C. Other variables, such as air temperature and resin-extractable NO_3^- did not vary significantly between seasons at all.

Lower montane forest is the only habitat that showed evidence of seasonal fluctuations in N_2O flux driven by variability in environmental conditions. This is evidenced by the results of multiple regression analysis of environmental variables against N_2O flux (section 5.3). Key variables found to influence N_2O flux included air temperature, soil temperature, WFPS, and resin-extractable NH_4^+ flux. According to the multiple regression analysis, the dominant environmental regulator for N_2O flux was air temperature, which showed a negative relationship with N_2O flux. While we are not entirely certain why air temperature was negatively correlated with flux; one possible explanation is that this relationship reflects the effect of air temperature on some other process linked to N_2O flux, such as drying of surface soil layers. Higher air temperatures may have led to increased evaporation in surface soil horizons, reducing rates of N cycling. This is a phenomenon we have observed in other warm, seasonally-dry environments (Teh et al., 2011), and we found limited evidence for this interpretation of the data in the weak but statistically significant inverse relationship between air temperature and WFPS (r^2 = 0.12, P < 0.002; data not shown). The positive relationship between soil temperature is perhaps more intuitive to interpret, and may reflect enhanced microbial activity as the soil warms. Likewise, the negative relationship with WFPS and N_2O flux probably reflects enhanced N_2O reductase activity and greater denitrification to N_2 with increasingly anaerobic conditions (Morley and Baggs, 2010;Morley et al., 2008). Last, the inverse relationship between resin-extractable NH_4^+ and N_2O flux may reflect competition for NO_3^- between denitrification and dissimilatory nitrate reduction to ammonium (DNRA), the two nitrate-reducing processes that are believed to be relatively common in wet, organic matter-rich tropical soils (Silver et al., 2001). Of course, one puzzling feature of this data is the divergent relationships that air temperature and soil temperature show with N_2O flux. We believe that the most likely explanation for this is that these two environmental variables are, to some extent, decoupled from each other in these montane habitats, leading to the two variables behaving differently from each other and acting as least quasi-independently on N_2O flux. This is evidenced by the weak positive correlation between air and soil temperature in lower montane forest (r^2 = 0.20, P < 0.0001), which suggests that a large proportion of the variance in soil temperatures (i.e. up to 80 %) are

explained by other environmental factors, and not by ambient air temperature alone. However, it is important to note that interpretation of these results must be treated with some caution, given that the model as a whole was only on the borderline of statistical significance ($P < 0.07$, $r^2 = 0.36$).

One other important difference between this publication and our earlier work is that topography no longer appears to be an important driving variable in this multi-annual dataset. While the basin landform showed significantly lower N_2O flux than the other landforms when the effect of topography was investigated in isolation, a more comprehensive statistical analysis, which included topography and other variables (e.g. habitat, season, environmental conditions), suggests that topography is not a significant predictor of N_2O flux. Instead, the effects of topography may be contingent upon or co-vary with habitat, rather than acting independently of it.

6.2 Effects of soil moisture on N_2O flux

Results from our laboratory-based WFPS manipulations suggest that soil moisture content plays a significant role in modulating N_2O flux. This finding is noteworthy because our prior research suggested that there was no direct relationship between N_2O flux and WFPS (Teh et al., 2014), and challenged our broader theoretical understanding of the role that soil moisture plays in regulating N_2O flux (Firestone and Davidson, 1989;Firestone et al., 1980;Weier et al., 1993). However, the response of ^{15}N-N_2O flux and other response variables (e.g. ^{15}N-N_2 flux, N_2O yield) were complex and non-linear, falsifying our second hypothesis (**H2**). Rather than ^{15}N-N_2O flux increasing progressively with WFPS, as predicted by **H2** and denitrification theory (Firestone and Davidson, 1989;Firestone et al., 1980;Weier et al., 1993), we observed two distinct and separate peaks in ^{15}N-N_2O flux. The highest ^{15}N-N_2O flux was observed in the 90 and 50 % WFPS treatments, while the 30 and 70 % WFPS treatments showed significantly lower flux (Fisher's LSD, $P < 0.05$; Figure 4). This unexpected result may reflect competition for substrates (e.g. NO_3^-, labile organic C) among nitrate-reducing processes such as denitrification and DNRA (Silver et al., 2001), or may indicate that N_2O is being produced from DNRA (Streminska et al., 2012).

^{15}N-N_2 flux and N_2O yield also showed intriguing and unexpected trends. For example, ^{15}N-N_2 flux was highest flux in the 90 % WFPS treatment (Fisher's LSD, P < 005), but did not differ significantly among the other treatments (Figure 4). Likewise, N_2O yield was highest in the 70 % WFPS treatment (0.51 ± 0.06), above and below which significantly smaller proportions of ^{15}N were emitted as N_2O (Fisher's LSD, P < 0.05). These results are surprising because denitrification theory predicts that decreases in WFPS should lead to a reduction in N_2 flux and increases in N_2O yield (Firestone and Davidson, 1989;Firestone et al., 1980;Weier et al., 1993), as N_2O reductase is increasingly suppressed by drier and more oxic soil conditions (Burgin and Groffman, 2012;Weier et al., 1993;Firestone et al., 1980;Morley and Baggs, 2010;Morley et al., 2008). One explanation for this is that N_2O production under drier conditions (i.e. <50 % WFPS) may be occurring in anaerobic microsites (Keller et al., 1993;Silver et al., 1999).

6.3 N_2O flux not constrained by labile organic matter availability

Nitrous oxide flux was unaffected by variations in leaf litter-fall, partially challenging our third hypothesis (**H3**). This finding runs counter to the results from lowland tropical forests (Sayer et al., 2011), where trace gas flux can be strongly influenced by changes in labile organic matter inputs, such as leaf litter. The relative insensitivity of these montane ecosystems to changes in leaf litter-fall, a proxy for labile organic matter inputs, may be due to the relatively large size of soil organic matter pools in these soils (Zimmermann et al., 2012, Zimmermann et al., 2009a, Zimmermann et al., 2010b), which could buffer N_2O production against short-term fluctuations in labile organic matter availability. Moreover, because of the relatively large soil organic matter stocks, and N_2O emission could be more strongly constrained by other factors, such as N availability, soil WFPS or pH. This finding is significant for understanding and modelling process-based controls on N_2O flux, as many bottom-up, process-based models assume that N cycling and turnover of labile organic matter are linked through processes such as litter production and decomposition (Li et al., 2000;Werner et al., 2007). While not disproving these assumptions, these data suggest that the linkage between litter production and N_2O flux are weak in these montane environments.

6.4 Importance of NO_3^- in regulating N_2O flux

One of the principal hypotheses raised by our earlier research is that N_2O flux is strongly limited by NO_3^- across this tropical elevation gradient (Teh et al., 2014). The detailed, process-oriented studies conducted here provide evidence that supports this claim, indicating that longer-term, time-averaged patterns in NO_3^- availability among habitats influence N_2O flux. The strongest evidence comes from the ^{15}N-N_2O flux data from our ^{15}N-NO_3^- addition experiment. Trends in ^{15}N-N_2O flux echoed patterns in our field data and prior denitrification potential experiments (Teh et al., 2014). Namely, we observed an inverse trend in ^{15}N-N_2O flux with elevation, with significantly higher ^{15}N-N_2O flux from lower elevation premontane (86 ± 16 ng N_2O-^{15}N g^{-1} d^{-1}) and lower montane (179 ± 48 ng N_2O-^{15}N g^{-1} d-1) forests, compared to higher elevation upper montane forest mineral layer soils (0.06 ± 0.01 ng N_2O-^{15}N g^{-1} d^{-1}) and montane grasslands (11 ± 4 ng N_2O-^{15}N g^{-1} d^{-1}) (Figure 5a). This pattern in ^{15}N-N_2O flux follows trends in resin-extractable NO_3^- flux, implying that NO_3^- may constrain the potential of these soil to emit N_2O (Figure 2a-b, Figure 5a) (Teh et al., 2014). The exception to this pattern is upper montane forest organic layer soils, which showed the highest flux when incubated under laboratory conditions (Figure 5). However, it is important to note that the significantly lower bulk density of the organic horizon in upper montane forests (~0.06 g cm^{-3} for the O horizon versus ~0.6 g cm^{-3} for the mineral horizon) means that this O layer makes a smaller proportional contribution to N_2O flux than soils from lower mineral horizons (Zimmermann et al., 2009a;Zimmermann et al., 2009b).

Furthermore, the behaviour of the NO_3^- amended soils during the early (≤24 hours) and late (>24 hours) phases of the incubation suggest that soils from more N-poor habitats showed a greater proportional increase in ^{15}N-N_2O flux following NO_3^- addition than N-rich habitats, suggesting that ^{15}N-N_2O flux was more NO_3^- limited in N-poor environments (Figure 5). For example, soils from the upper montane forest organic layer, montane grasslands, and upper montane forest mineral layer showed the lowest early phase ^{15}N-N_2O flux, but the greatest proportional increase in flux during the late incubation phase, rising by a factor of 59, five, and two, respectively. In contrast, lower montane and premontane forest soils, which showed the highest NO_3^- availability and N_2O flux in the field, and the greatest early phase ^{15}N-N_2O flux in the incubations, showed the smallest proportional increase in the late incubation phase (i.e. 1.7 times increase). Overall, these data imply that ^{15}N-N_2O flux from N-

poor habitats are more strongly NO_3^- limited, whereas N_2O flux from more N-rich soils may be more heavily constrained by other environmental factors.

The other field and laboratory data were more equivocal, reflecting the complex and potentially confounding environmental controls on N_2O flux (Groffman et al., 2009). For example, while lower N_2O flux was associated with more N-poor habitats, N_2O flux was only weakly correlated with resin-extractable NO_3^- flux (r^2 = 0.03, P <0.03). Moreover, for the laboratory-based NO_3^- addition experiment, we found no evidence that these soils responded to short-term increases in NO_3^- availability, at least within the concentration range that we used in this experiment. ^{15}N-N_2O flux, ^{15}N-N_2 flux, and N_2O yield were not directly influenced by the amount of ^{15}N-NO_3^- added (Figure 5). Rather, ANCOVA suggests that ^{15}N-N_2O and ^{15}N-N_2 fluxes were better-predicted by habitat. N_2O yield, normally a sensitive indicator of NO_3^- availability (Blackmer and Bremner, 1978;Weier et al., 1993;Parton et al., 1996), showed no immediate response to the amount of ^{15}N-NO_3^- added, nor any of the other explanatory variables. One explanation for this, consistent with the notion that N_2O flux is NO_3^- limited, is that nitrate-reducing microbes in these soils may have a relatively low half-saturation constant (K_m) for NO_3^-, and effectively utilize NO_3^- whenever concentrations increase above background levels (Holtan-Hartwig et al., 2000). As a consequence, we may be unable to differentiate among NO_3^- treatments because the NO_3^- addition levels that we used all exceeded the K_m for in these soils. This finding is also consistent with results from long-term N fertilization studies, which suggest that substantive shifts in N_2O flux are only likely to occur after prolonged exposure to high levels of N, rather than due to transient fluctuations in N availability (Hall & Matson 1993; Koehler et al 2009; Corre et al 2014).

7. Conclusions

Process-based studies of N_2O flux from montane tropical ecosystems in the southern Peruvian Andes affirms prior research suggesting that these ecosystems are potentially important regional sources of N_2O (Teh et al., 2014). Nitrous oxide flux originated primarily from nitrate reduction rather than from nitrification, probably due to low pH soil conditions. Contrary to our earlier research, we found only weak evidence for seasonal patterns in N_2O

flux, with the exception of lower montane forest, which showed significantly higher N_2O flux during the dry season compared to the wet season. Weak seasonal trends in N_2O flux among the other montane habitats probably stems from relatively modest variation in key environmental drivers (e.g. temperature, WFPS, NO_3^-) between seasons. Nitrous oxide flux was significantly influenced by soil moisture content, but the effect of soil moisture content on N_2O flux was complex and non-linear. Nitrous oxide flux showed a bimodal response to increasing soil moisture content, with peaks in N_2O flux at 90 and 50 % WFPS. These data suggest that the effects of water on N_2O flux are complicated by other factors, such as competition for substrates among different nitrate-reducing processes, or shifts in the amount of N_2O derived from denitrification or DNRA. Substrate manipulation experiments indicated that N_2O flux was limited by NO_3^-, but unconstrained by the input rate of labile organic matter (i.e. leaf litter). Nitrous oxide flux was relatively insensitive to short-term variations in NO_3^-, and was better-predicted by longer-term, time-averaged variations in NO_3^- availability.

8. Author Contributions

TD designed the field and laboratory experiments, collected the field data, conducted the laboratory experiments, processed the samples, analysed the data, and contributed to the preparation of the manuscript. NJM contributed to the design of the laboratory experiments, assisted in the sample analysis, assisted in the analysis of the laboratory data, and contributed to the preparation of the manuscript. AJC and LPHQ assisted in the collection of the field data and processing of the field samples. EMB, PM, MR, and PS contributed to the experimental design and the preparation of the manuscript. YAT directed the research, contributed to the design of the experiments, assisted in the analysis of the field and laboratory data, and took the principal role in preparing the manuscript.

9. Acknowledgements

The authors would like to acknowledge the agencies that funded this research; the UK Natural Environment Research Council (NERC; joint grant references NE/H006583, NE/H007849 and NE/H006753). Patrick Meir was supported by an Australian Research

Council Fellowship (FT110100457). Javier Eduardo Silva Espejo, Walter Huaraca Huasco, and the ABIDA NGO provided critical fieldwork and logistical support. Angus Calder (University of St Andrews) and Vicky Munro (University of Aberdeen) provided invaluable laboratory support. Thanks to Adrian Tejedor from the Amazon Conservation Association, who provided assistance with site access and site selection at Hacienda Villa Carmen. This publication is a contribution from the Scottish Alliance for Geoscience, Environment and Society (http://www.sages.ac.uk).

10. References

Baggs, E. M., Richter, M., Hartwig, U.A., and Cadisch, G. : Nitrous oxide emissions from grass swards during the eighth year of elevated atmospheric pCO2 (Swiss FACE). , Global Change Biology 9, 1214-1222., 2003.

Bateman, E. J., and Baggs, E. M.: Contributions of nitrification and denitrification to N2O emissions from soils at different water-filled pore space, Biology and Fertility of Soils, 41, 379-388, 10.1007/s00374-005-0858-3, 2005.

Belyea, L. R., and Baird, A. J.: Beyond "The limits to peat bog growth": Cross-scale feedback in peatland development, Ecological Monographs, 76, 299-322, 2006.

Blackmer, A. M., and Bremner, J. M.: Inhibitory effect of nitrate on reduction of N2O to N2 by soil microorganisms, Soil Biology and Biochemistry, 10, 187-191, http://dx.doi.org/10.1016/0038-0717(78)90095-0, 1978.

Breuer, L., Papen, H., and Butterbach-Bahl, K.: N2O emission from tropical forest soils of Australia, J. Geophys. Res.-Atmos., 105, 26353-26367, 10.1029/2000jd900424, 2000.

Burgin, A. J., and Groffman, P. M.: Soil O2 controls denitrification rates and N2O yield in a riparian wetland, Journal of Geophysical Research: Biogeosciences, 117, n/a-n/a, 10.1029/2011JG001799, 2012.

Corre, M. D., Veldkamp, E., Arnold, J., and Wright, S. J.: Impact of elevated N input on soil N cycling and losses in old-growth lowland and montane forests in Panama, Ecology, 91, 1715-1729, 10.1890/09-0274.1, 2010.

Davidson, E. A.: Fluxes of nitrous oxide and nitric oxide from terrestrial ecosystems, in: Microbial production and consumption of greenhouse gases: methane, nitrogen oxides, and

halomethanes., edited by: Rogers, J. E., and Whitman, W. B., American Society for Microbiology, Washington D.C., 219-236, 1991.

Eva, H. D., Belward, A. S., De Miranda, E. E., Di Bella, C. M., Gond, V., Huber, O., Jones, S., Sgrenzaroli, M., and Fritz, S.: A land cover map of South America, Global Change Biology, 10, 731-744, 10.1111/j.1529-8817.2003.00774.x, 2004.

Firestone, M. K., Firestone, R. B., and Tiedge, J. M.: Nitrous oxide from soil denitrification: Factors controlling its biological production., Science, 208, 749-751, 1980.

Firestone, M. K., and Davidson, E. A.: Microbiological basis of NO and N2O production and consumption in soil, in: Exchange of Trace Gases Between Terrestrial Ecosystems and the Atmosphere, edited by: Andrae, M. O., and Schimel, D. S., John Wiley and Sons Ltd., New York, 7-21, 1989.

Girardin, C. A. J., Malhi, Y., AragÃO, L. E. O. C., Mamani, M., Huaraca Huasco, W., Durand, L., Feeley, K. J., Rapp, J., Silva-Espejo, J. E., Silman, M., Salinas, N., and Whittaker, R. J.: Net primary productivity allocation and cycling of carbon along a tropical forest elevational transect in the Peruvian Andes, Global Change Biology, 16, 3176-3192, 10.1111/j.1365-2486.2010.02235.x, 2010.

Groffman, P. M., Butterbach-Bahl, K., Fulweiler, R. W., Gold, A. J., Morse, J. L., Stander, E. K., Tague, C., Tonitto, C., and Vidon, P.: Challenges to incorporating spatially and temporally explicit phenomena (hotspots and hot moments) in denitrification models, Biogeochemistry, 93, 49-77, 10.1007/s10533-008-9277-5, 2009.

Hirsch, A. I., Michalak, A. M., Bruhwiler, L. M., Peters, W., Dlugokencky, E. J., and Tans, P. P.: Inverse modeling estimates of the global nitrous oxide surface flux from 1998-2001, Global Biogeochemical Cycles, 20, 1-17, Gb1008 10.1029/2004gb002443, 2006.

Holtan-Hartwig, L., Dorsch, P., and Bakken, L. R.: Comparison of denitrifying communities in organic soils: kinetics of NO3- and N2O reduction, Soil Biol. Biochem., 32, 833-843, 10.1016/s0038-0717(99)00213-8, 2000.

Huang, J., Golombek, A., Prinn, R., Weiss, R., Fraser, P., Simmonds, P., Dlugokencky, E. J., Hall, B., Elkins, J., Steele, P., Langenfelds, R., Krummel, P., Dutton, G., and Porter, L.: Estimation of regional emissions of nitrous oxide from 1997 to 2005 using multinetwork measurements, a chemical transport model, and an inverse method, J. Geophys. Res.-Atmos., 113, 1-19, D17313

10.1029/2007jd009381, 2008.

Jones, S. P., Diem, T., Huaraca Quispe, L. P., Cahuana, A. J., Reay, D. S., Meir, P., and Teh, Y. A.: Drivers of atmospheric methane uptake by montane forest soils in the southern Peruvian Andes, Biogeosciences, 13, 4151-4165, 10.5194/bg-13-4151-2016, 2016.

Keller, M., Veldkamp, E., Weltz, A., and Reiners, W.: Effect of pasture age on soil trace-gas emissions from a deforested area of Costa Rica., Nature, 365, 244-246, 1993.

Kort, E. A., Patra, P. K., Ishijima, K., Daube, B. C., Jimenez, R., Elkins, J., Hurst, D., Moore, F. L., Sweeney, C., and Wofsy, S. C.: Tropospheric distribution and variability of N2O: Evidence for strong tropical emissions, Geophys. Res. Lett., 38, 5, 10.1029/2011gl047612, 2011.

Li, C., Aber, J., Stange, F., Butterbach-Bahl, K., and Papen, H.: A process-oriented model of N2O and NO emissions from forest soils: 1. Model development, Journal of Geophysical Research: Atmospheres, 105, 4369-4384, 10.1029/1999JD900949, 2000.

Limmer, A. W., and Steele, K. W.: Denitrification potentials: Measurement of seasonal variation using a short-term anaerobic incubation technique, Soil Biology and Biochemistry, 14, 179-184, http://dx.doi.org/10.1016/0038-0717(82)90020-7, 1982.

Livingston, G., and Hutchinson, G.: Chapter 2: Enclosure-based measurement of trace gas exchange: applications and sources of error., in: Biogenic Trace Gases: Measuring Emissions from Soil and Water., edited by: Matson, P., Harriss, RC, Blackwell Science Ltd, Cambridge, MA, USA, 14-51, 1995.

Malhi, Y., Silman, M., Salinas, N., Bush, M., Meir, P., and Saatchi, S.: Introduction: Elevation gradients in the tropics: laboratories for ecosystem ecology and global change research, Global Change Biology, 16, 3171-3175, 10.1111/j.1365-2486.2010.02323.x, 2010.

Morley, N., Baggs, E. M., Dörsch, P., and Bakken, L.: Production of NO, N2O and N2 by extracted soil bacteria, regulation by NO2− and O2 concentrations, FEMS Microbiol. Ecol., 65, 102-112, 10.1111/j.1574-6941.2008.00495.x, 2008.

Morley, N., and Baggs, E. M.: Carbon and oxygen controls on N2O and N-2 production during nitrate reduction, Soil Biol. Biochem., 42, 1864-1871, 10.1016/j.soilbio.2010.07.008, 2010.

Moser, G., Leuschner, C., Hertel, D., Graefe, S., Soethe, N., and Iost, S.: Elevation effects on the carbon budget of tropical mountain forests (S Ecuador): the role of the belowground compartment, Global Change Biology, 17, 2211-2226, 10.1111/j.1365-2486.2010.02367.x, 2011.

Nevison, C. D., Lueker, T. J., and Weiss, R. F.: Quantifying the nitrous oxide source from coastal upwelling, Global Biogeochemical Cycles, 18, 24, Gb1018 10.1029/2003gb002110, 2004.

Nevison, C. D., Mahowald, N. M., Weiss, R. F., and Prinn, R. G.: Interannual and seasonal variability in atmospheric N2O, Global Biogeochemical Cycles, 21, GB3017, 10.1029/2006GB002755, 2007.

Parton, W. J., Mosier, A. R., Ojima, D. S., Valentine, D. W., Schimel, D. S., Weier, K., and Kulmala, A. E.: Generalized model for N2 and N2O production from nitrification and denitrification, Global Biogeochemical Cycles, 10, 401-412, 10.1029/96GB01455, 1996.

Pedersen, A. R., Petersen, S. O., and Schelde, K.: A comprehensive approach to soil-atmosphere trace-gas flux estimation with static chambers, European Journal of Soil Science, 61, 888-902, 10.1111/j.1365-2389.2010.01291.x, 2010.

Potter, C. S., Matson, P. A., Vitousek, P. M., and Davidson, E. A.: Process modeling of controls on nitrogen trace gas emissions from soils worldwide, Journal of Geophysical Research: Atmospheres, 101, 1361-1377, 10.1029/95JD02028, 1996.

Pumpanen, J., Kolari, P., Ilvesniemi, H., Minkkinen, K., Vesala, T., Niinistö, S., Lohila, A., Larmola, T., Morero, M., Pihlatie, M., Janssens, I., Yuste, J. C., Grünzweig, J. M., Reth, S., Subke, J.-A., Savage, K., Kutsch, W., Østreng, G., Ziegler, W., Anthoni, P., Lindroth, A., and Hari, P.: Comparison of different chamber techniques for measuring soil CO2 efflux, Agric. For. Meteorol., 123, 159-176, http://dx.doi.org/10.1016/j.agrformet.2003.12.001, 2004.

R Core Team: A language and environment for statistical computing, R Foundation for Statistical Computing, Vienna, Austria, 2012.

Saikawa, E., Schlosser, C. A., and Prinn, R. G.: Global modeling of soil nitrous oxide emissions from natural processes, Global Biogeochemical Cycles, 27, 972-989, 10.1002/gbc.20087, 2013.

Saikawa, E., Prinn, R. G., Dlugokencky, E., Ishijima, K., Dutton, G. S., Hall, B. D., Langenfelds, R., Tohjima, Y., Machida, T., Manizza, M., Rigby, M., O'Doherty, S., Patra, P. K., Harth, C. M., Weiss, R. F., Krummel, P. B., van der Schoot, M., Fraser, P. J., Steele, L. P., Aoki, S., Nakazawa, T., and Elkins, J. W.: Global and regional emissions estimates for N2O, Atmospheric Chemistry and Physics, 14, 4617-4641, 10.5194/acp-14-4617-2014, 2014.

Sayer, E. J., Heard, M. S., Grant, H. K., Marthews, T. R., and Tanner, E. V. J.: Soil carbon release enhanced by increased tropical forest litterfall, Nature Clim. Change, 1, 304-307,

http://www.nature.com/nclimate/journal/v1/n6/abs/nclimate1190.html - supplementary-information, 2011.

Silver, W., Lugo, A., and Keller, M.: Soil oxygen availability and biogeochemistry along rainfall and topographic gradients in upland wet tropical forest soils., Biogeochemistry, 44, 301-328, 1999.

Silver, W. L., Herman, D. J., and Firestone, M. K. S.: Dissimilatory Nitrate Reduction to Ammonium in Upland Tropical Forest Soils., Ecology, 82, 2410-2416, 2001.

Streminska, M. A., Felgate, H., Rowley, G., Richardson, D. J., and Baggs, E. M.: Nitrous oxide production in soil isolates of nitrate-ammonifying bacteria, Environ. Microbiol. Rep., 4, 66-71, 10.1111/j.1758-2229.2011.00302.x, 2012.

Subler, S., Blair, J. M., and Edwards, C. A.: Using anion-exchange membranes to measure soil nitrate availability and net nitrification, Soil Biology and Biochemistry, 27, 911-917, http://dx.doi.org/10.1016/0038-0717(95)00008-3, 1995.

Teh, Y. A., Silver, W. L., Sonnentag, O., Detto, M., Kelly, M., and Baldocchi, D. D.: Large Greenhouse Gas Emissions from a Temperate Peatland Pasture, Ecosystems, 14, 311-325, 10.1007/s10021-011-9411-4, 2011.

Teh, Y. A., Diem, T., Jones, S., Huaraca Quispe, L. P., Baggs, E., Morley, N., Richards, M., Smith, P., and Meir, P.: Methane and nitrous oxide fluxes across an elevation gradient in the tropical Peruvian Andes, Biogeosciences, 11, 2325-2339, 10.5194/bg-11-2325-2014, 2014.

Templer, P. H., Lovett, G. M., Weathers, K. C., Findlay, S. E., and Dawson, T. E.: Influence of tree species on forest nitrogen retention in the Catskill Mountains, New York, USA, Ecosystems, 8, 1-16, 10.1007/s10021-004-0230-8, 2005.

Varner, R. K., Keller, M., Robertson, J. R., Dias, J. D., Silva, H., Crill, P. M., McGroddy, M., and Silver, W. L.: Experimentally induced root mortality increased nitrous oxide emission from tropical forest soils, Geophys. Res. Lett., 30, n/a-n/a, 10.1029/2002GL016164, 2003.

Veldkamp, E., Purbopuspito, J., Corre, M. D., Brumme, R., and Murdiyarso, D.: Land use change effects on trace gas fluxes in the forest margins of Central Sulawesi, Indonesia, Journal of Geophysical Research-Biogeosciences, 113, 1-11, G02003 10.1029/2007jg000522, 2008.

Weier, K. L., Doran, J. W., Power, J. F., and Walters, D. T.: Denitrification and the denitrogen nitrous oxide ratio as affected by soil water, available carbon, and nitrate, Soil Sci. Soc. Am. J., 57, 66-72, 1993.

Werner, C., Butterbach-Bahl, K., Haas, E., Hickler, T., and Kiese, R.: A global inventory of N2O emissions from tropical rainforest soils using a detailed biogeochemical model, Global Biogeochemical Cycles, 21, 1-18, Gb3010 10.1029/2006gb002909, 2007.

Wolf, K., Veldkamp, E., Homeier, J., and Martinson, G. O.: Nitrogen availability links forest productivity, soil nitrous oxide and nitric oxide fluxes of a tropical montane forest in southern Ecuador, Global Biogeochemical Cycles, 25, GB4009, 10.1029/2010GB003876, 2011.

Wolf, K., Flessa, H., and Veldkamp, E.: Atmospheric methane uptake by tropical montane forest soils and the contribution of organic layers, Biogeochemistry, 111, 469-483, 10.1007/s10533-011-9681-0, 2012.

Zimmermann, M., Meir, P., Bird, M., Malhi, Y., and Ccahuana, A.: Litter contribution to diurnal and annual soil respiration in a tropical montane cloud forest, Soil Biology and Biochemistry, 41, 1338-1340, 2009a.

Zimmermann, M., Meir, P., Bird, M. I., Malhi, Y., and Ccahuana, A. J. Q.: Climate dependence of heterotrophic soil respiration from a soil-translocation experiment along a 3000 m tropical forest altitudinal gradient, European Journal of Soil Science, 60, 895-906, 10.1111/j.1365-2389.2009.01175.x, 2009b.

Biogeosciences Discuss., doi:10.5194/bg-2017-107, 2017
Manuscript under review for journal Biogeosciences
Discussion started: 30 March 2017

12. Tables and Figures

Table 1. Site characteristics.

Elevation Band m a.s.l.	Habitat	Latitude	Longitude	Mean Annual Temperature Soil 0-10 cm °C	Mean Annual Precipitation mm	Bulk density 0-10 cm g cm-3	pH	Soil C/N 0-10 cm	Soil C 0-10 cm %	Mineral Soil Particle Size 0-10 cm Clay	Silt	Sand	10-30 cm Clay	Silt	Sand	Landforms	Plots n	Flux Chambers n
600-1200	Premontane forest	12°53'43"	71°23'04"	20.5	5318	0.38 ± 0.03 (n = 21)	3.4 ± 0.1	11.3 ± 0.2	7.9 ± 0.5	5.4 ± 0.3	68.8 ± 3.9	25.4 ± 15.9	8.9 ± 1.8	81.0 ± 1.7	10.3 ± 2.5	ridge, slope, flat	3	15
200-2200	Lower montane forest	13°2'56"	71°32'13"	17.2	2631	0.19 ± 0.03 (n = 17)	3.4 ± 0.1	14.5 ± 0.2	25.2 ± 1.3	3.6 ± 0.4	67.3 ± 4.2	29.3 ± 4.5	7.2 ± 0.4	83.8 ± 0.8	9.0 ± 0.9	ridge, slope, flat	3	15
200-3200	Upper montane forest	13°11'24"	71°35'13"	10.7	1706	0.41 ± 0.02 (n = 12)	3.9 ± 0.1	16.8 ± 0.4	16.3 ± 1.0	5.1 ± 0.9	57.1 ± 7.9	37.9 ± 8.7	4.4 ± 2.0	46.5 ± 16.2	49.1 ± 18.1	ridge, slope	3	15
200-3700	Montane grassland	13°07'19"	71°36'54"	9.3	2200	0.36 ± 0.03 (n = 27)	4.1 ± 0.1	12.9 ± 0.4	16.0 ± 1.0	2.6 ± 0.2	54.4 ± 3.0	43.0 ± 3.2	n/a	n/a	n/a	ridge, slope, flat, basin	4	20

Biogeosciences Discuss., doi:10.5194/bg-2017-107, 2017
Manuscript under review for journal Biogeosciences
Discussion started: 30 March 2017

Table 2. Description of the water-filled pore space and NO_3^- addition treatments for the laboratory manipulation experiments.

Habitat	Experimental Treatment	Soil Depth	Soil Type	WFPS %	Inorganic N added µg N (g soil)$^{-1}$	^{15}N Tracer	Replicate n
WATER-FILLED PORE SPACE							
Premontane forest	90 % WFPS	0-10	mineral	90	200	$^{15}NH_4^{15}NO_3$	5
	90 % WFPS	0-10	mineral	90	200	$^{14}NH_4^{15}NO_3$	5
	70 % WFPS	0-10	mineral	70	200	$^{15}NH_4^{15}NO_3$	5
	70 % WFPS	0-10	mineral	70	200	$^{14}NH_4^{15}NO_3$	5
	50 % WFPS	0-10	mineral	50	200	$^{15}NH_4^{15}NO_3$	5
	50 % WFPS	0-10	mineral	50	200	$^{14}NH_4^{15}NO_3$	5
	30 % WFPS	0-10	mineral	30	200	$^{15}NH_4^{15}NO_3$	5
	30 % WFPS	0-10	mineral	30	200	$^{14}NH_4^{15}NO_3$	5
Lower montane forest	90 % WFPS	0-10	mineral	90	200	$^{15}NH_4^{15}NO_3$	5
	90 % WFPS	0-10	mineral	90	200	$^{14}NH_4^{15}NO_3$	5
	70 % WFPS	0-10	mineral	70	200	$^{15}NH_4^{15}NO_3$	5
	70 % WFPS	0-10	mineral	70	200	$^{14}NH_4^{15}NO_3$	5
	50 % WFPS	0-10	mineral	50	200	$^{15}NH_4^{15}NO_3$	5
	50 % WFPS	0-10	mineral	50	200	$^{14}NH_4^{15}NO_3$	5
	30 % WFPS	0-10	mineral	30	200	$^{15}NH_4^{15}NO_3$	5
	30 % WFPS	0-10	mineral	30	200	$^{14}NH_4^{15}NO_3$	5
Upper montane forest	90 % WFPS	10-20	mineral	90	20	$^{15}NH_4^{15}NO_3$	5
	90 % WFPS	10-20	mineral	90	20	$^{14}NH_4^{15}NO_3$	5
	70 % WFPS	10-20	mineral	70	20	$^{15}NH_4^{15}NO_3$	5
	70 % WFPS	10-20	mineral	70	20	$^{14}NH_4^{15}NO_3$	5
	50 % WFPS	10-20	mineral	50	20	$^{15}NH_4^{15}NO_3$	5
	50 % WFPS	10-20	mineral	50	20	$^{14}NH_4^{15}NO_3$	5
	30 % WFPS	10-20	mineral	30	20	$^{15}NH_4^{15}NO_3$	5
	30 % WFPS	10-20	mineral	30	20	$^{14}NH_4^{15}NO_3$	5
Montane grassland	90 % WFPS	0-10	mineral	90	20	$^{15}NH_4^{15}NO_3$	5
	90 % WFPS	0-10	mineral	90	20	$^{14}NH_4^{15}NO_3$	5
	70 % WFPS	0-10	mineral	70	20	$^{15}NH_4^{15}NO_3$	5
	70 % WFPS	0-10	mineral	70	20	$^{14}NH_4^{15}NO_3$	5
	50 % WFPS	0-10	mineral	50	20	$^{15}NH_4^{15}NO_3$	5
	50 % WFPS	0-10	mineral	50	20	$^{14}NH_4^{15}NO_3$	5
	30 % WFPS	0-10	mineral	30	20	$^{15}NH_4^{15}NO_3$	5
	30 % WFPS	0-10	mineral	30	20	$^{14}NH_4^{15}NO_3$	5
NITRATE ADDITION							
Premontane forest	control	0-10	mineral	80	n/a	n/a	5
	+50 % background NO_3^-	0-10	mineral	80	78 ± 6	$K^{15}NO_3$	5
	+100 % background NO_3^-	0-10	mineral	80	157 ± 12	$K^{15}NO_3$	5
	+150 % background NO_3^-	0-10	mineral	80	235 ± 17	$K^{15}NO_3$	5
Lower montane forest	control	0-10	mineral	80	n/a	n/a	5
	+50 % background NO_3^-	0-10	mineral	80	70 ± 6	$K^{15}NO_3$	5
	+100 % background NO_3^-	0-10	mineral	80	140 ± 12	$K^{15}NO_3$	5
	+150 % background NO_3^-	0-10	mineral	80	210 ± 18	$K^{15}NO_3$	5
Upper montane forest	control	0-10	organic	80	n/a	n/a	5
	+50 % background NO_3^-	0-10	organic	80	9 ±2	$K^{15}NO_3$	5
	+100 % background NO_3^-	0-10	organic	80	18 ± 5	$K^{15}NO_3$	5
	+150 % background NO_3^-	0-10	organic	80	27± 7	$K^{15}NO_3$	5
	control	10-20	mineral	80	n/a	n/a	5
	+50 % background NO_3^-	10-20	mineral	80	9 ± 4	$K^{15}NO_3$	5
	+100 % background NO_3^-	10-20	mineral	80	19 ± 7	$K^{15}NO_3$	5
	+150 % background NO_3^-	10-20	mineral	80	28 ± 11	$K^{15}NO_3$	5
Montane grassland	control	0-10	mineral	80	n/a	n/a	5
	+50 % background NO_3^-	0-10	mineral	80	3 ± 1	$K^{15}NO_3$	5
	+100 % background NO_3^-	0-10	mineral	80	6 ± 2	$K^{15}NO_3$	5
	+150 % background NO_3^-	0-10	mineral	80	9 ± 4	$K^{15}NO_3$	5

Biogeosciences Discuss., doi:10.5194/bg-2017-107, 2017
Manuscript under review for journal Biogeosciences
Discussion started: 30 March 2017

Table 3. Net N_2O flux and abiotic environmental variables for each habitat for the wet and dry season. Lower case letters indicate difference among seasons within habitats (*t*-Test on Box-Cox transformed data, $P < 0.05$). Values reported here are means and standard errors.

Habitat	N_2O mg N-N_2O m^{-2} d^{-1}		WFPS %		Soil Temperature °C		Air Temperature °C		Oxygen %		NO_3^- µg N-NO_3^- (g resin)$^{-1}$ d^{-1}		NH_4+ µg N-NH_4^+ (g resin)$^{-1}$ d^{-1}	
	Wet Season	Dry Season	Wet Season	Dry Season	Wet Season	Dry Season	Wet Season	Dry Season	Wet Season	Dry Season	Wet Season	Dry Season	Wet Season	Dry Season
Premontane	0.71 ± 0.25 a n = 130	0.79 ± 0.26 a n = 98	51.9 ± 1.6 a n = 135	51.2 ± 2.1 a n = 135	20.7 ± 0.1 a n = 143	20.2 ± 0.1 b n = 120	21.5 ± 0.3 n = 143	20.4 ± 0.5 n = 120	19.4 ± 0.2 a n = 52	19.6 ± 0.2 a n = 36	23.2 ± 3.6 a n = 89	22.1 ± 2.1 a n = 96	31.4 ± 13.0 n = 90	11.3 ± 1.8 n = 95
Lower montane	0.09 ± 0.08 a n = 212	1.02 ± 0.58 b n = 137	42.2 ± 1.0 a n = 271	34.0 ± 1.4 b n = 179	18.1 ± 0.1 a n = 254	17.3 ± 0.2 b n = 164	18.9 ± 0.3 n = 254	18.3 ± 0.2 n = 164	19.2 ± 0.2 a n = 146	19.2 ± 0.1 a n = 81	11.8 ± 1.9 a n = 123	7.8 ± 1.4 a n = 94	20.2 ± 5.4 n = 124	8.6 ± 0.9 n = 93
Upper montane	0.06 ± 0.09 a n = 207	0.01 ± 0.11 a n = 146	42.0 ± 1.3 a n = 264	24.3 ± 1.4 b n = 180	11.8 ± 0.1 a n = 255	10.9 ± 0.2 b n = 165	12.8 ± 0.2 n = 255	12.5 ± 0.3 n = 165	18.7 ± 0.2 a n = 165	18.5 ± 0.2 a n = 109	1.4 ± 0.2 a n = 128	0.6 ± 0.2 b n = 91	22.5 ± 6.3 n = 129	11.3 ± 1.4 n = 93
Montane grassland	-0.01 ± 0.11 a n = 238	0.19 ± 0.12 a n = 160	88.5 ± 0.3 a n = 303	88.3 ± 0.5 a n = 184	11.6 ± 0.1 a n = 282	9.0 ± 0.2 b n = 205	11.4 ± 0.3 n = 284	12.0 ± 0.5 n = 205	12.2 ± 0.9 a n = 176	15.4 ± 0.8 b n = 117	1.5 ± 0.4 a n = 128	2.1 ± 0.4 a n = 81	17.8 ± 4.3 n = 135	7.2 ± 0.8 n = 84

Biogeosciences Discuss., doi:10.5194/bg-2017-107, 2017
Manuscript under review for journal Biogeosciences
Discussion started: 30 March 2017

Figure 1. Map of study sites across the Kosñipata Valley, Manu National Park, Peru.

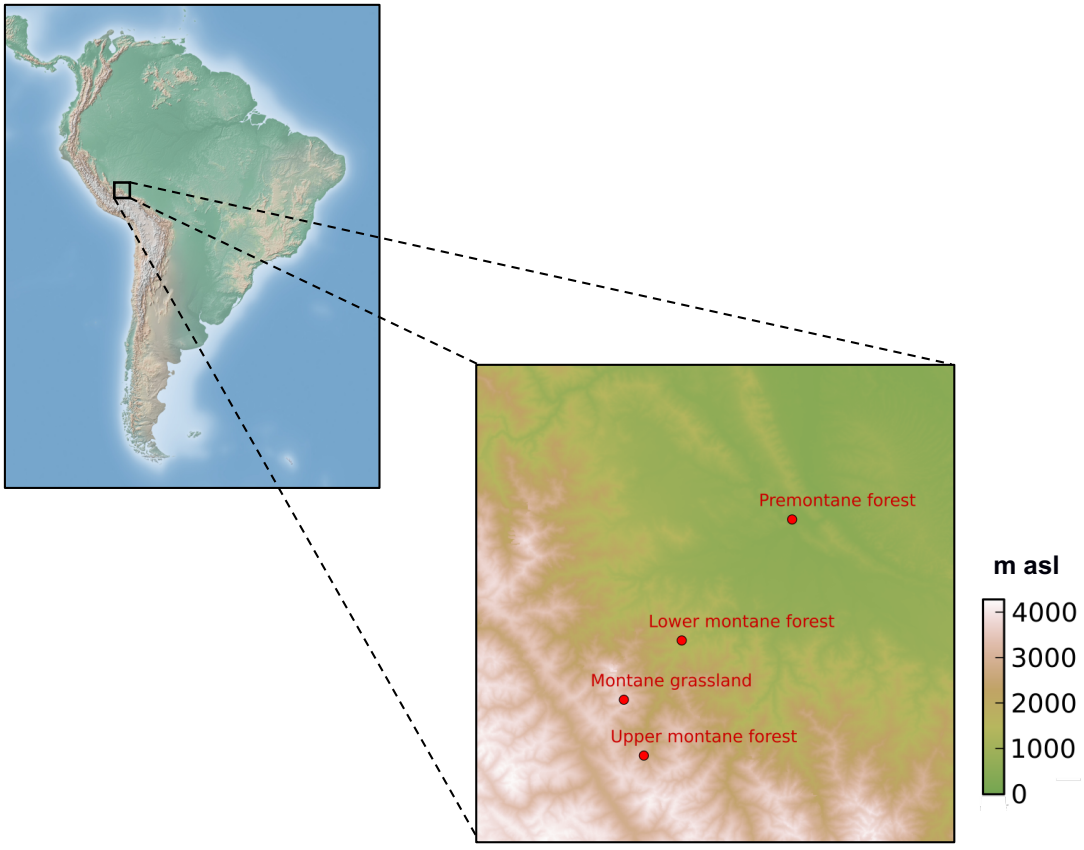

Biogeosciences Discuss., doi:10.5194/bg-2017-107, 2017
Manuscript under review for journal Biogeosciences
Discussion started: 30 March 2017

Figure 2. Plot-averaged (a) net N_2O flux, (b) water-filled pore space, and (c) resin-extractable NO_3^- flux among habitats. Boxes enclose the interquartile range, whiskers indicate the 90th and 10th percentiles. Lower case letters indicate statistically significant differences among means (Fisher's LSD, $P < 0.05$).

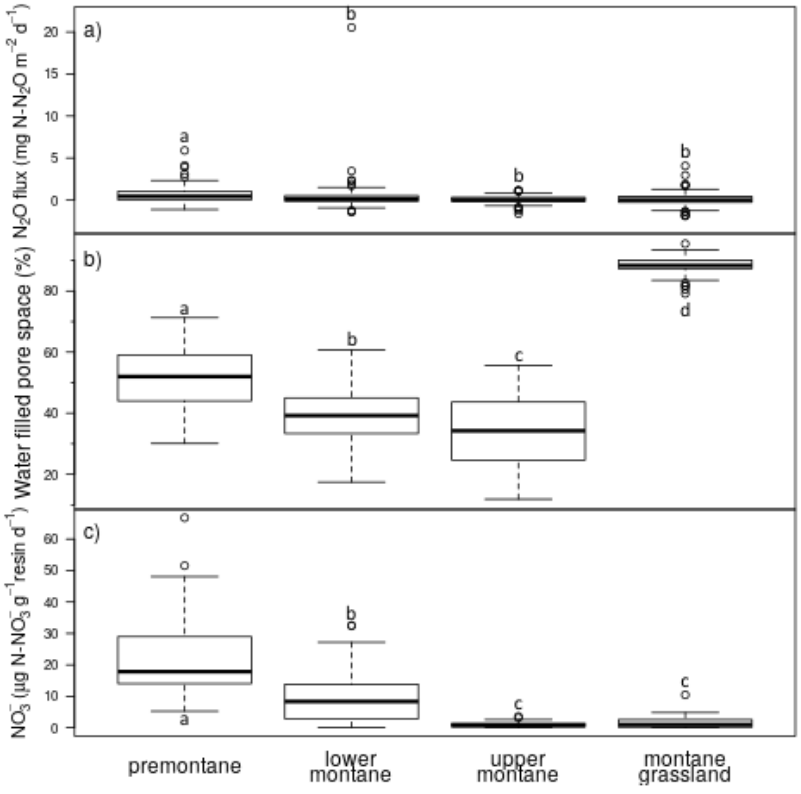

Biogeosciences Discuss., doi:10.5194/bg-2017-107, 2017
Manuscript under review for journal Biogeosciences
Discussion started: 30 March 2017

Figure 3. Time series of net N_2O flux and water-filled pore space (WFPS) for the whole data. Panels indicate data for (a) premontane forest, (b) lower montane forest, (c) upper montane forest, and (d) montane grasslands for the 30-month study period beginning in January 2011 and ending in June 2013. The broken horizontal line running across each panel denotes the overall mean N_2O flux or WFPS for that habitat. The broken line in each box indicate median values and the black lines indicate means. Dry and wet seasons are denoted by vertical shading on the graph, with the dry season (May to September) identified in white and the wet season (October to April) in light blue.

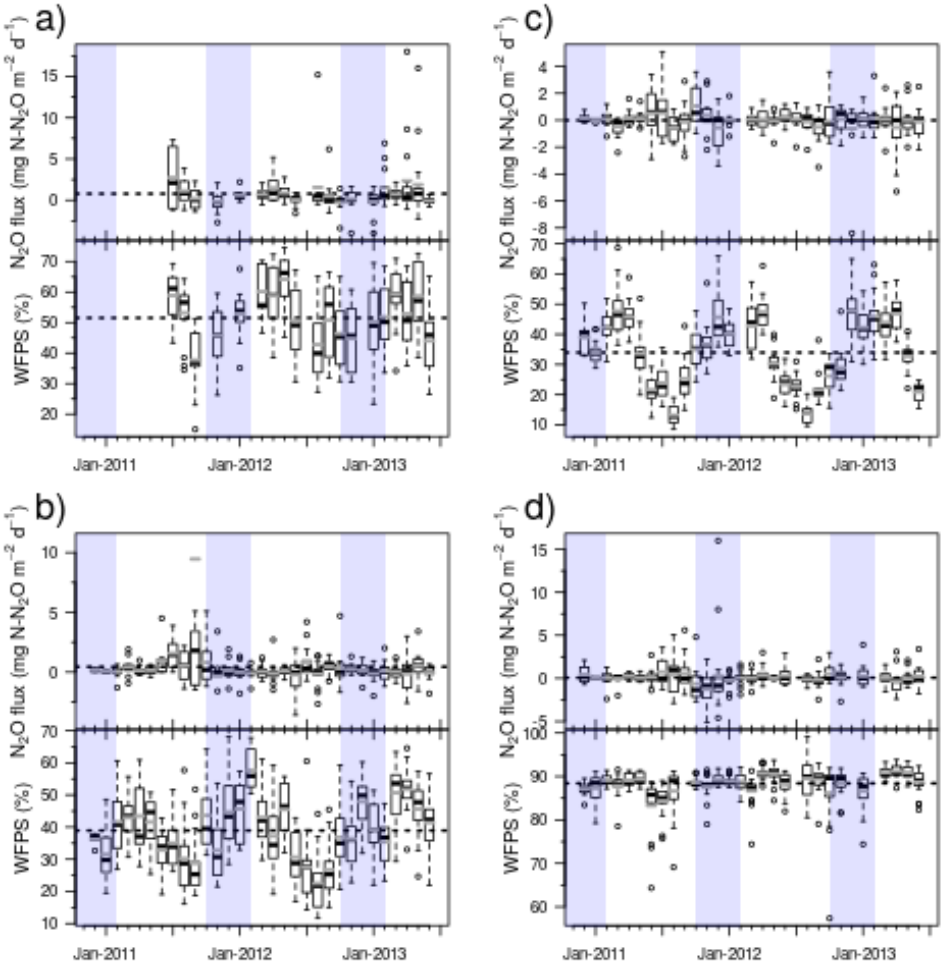

Biogeosciences Discuss., doi:10.5194/bg-2017-107, 2017
Manuscript under review for journal Biogeosciences
Discussion started: 30 March 2017

Figure 4. Total (a) ^{15}N-N_2O flux and (b) ^{15}N-N_2 flux during the early (≤24 hours) and late (>24 hours) incubation phases of the water-filled pore space (WFPS) experiment. Results from the 90 % WFPS treatment are shown in dark-grey, while data from the 70 %, 50 %, and 30 % treatments are shown in mid-grey, light-grey, and white, respectively. The bar charts show means and standard errors.

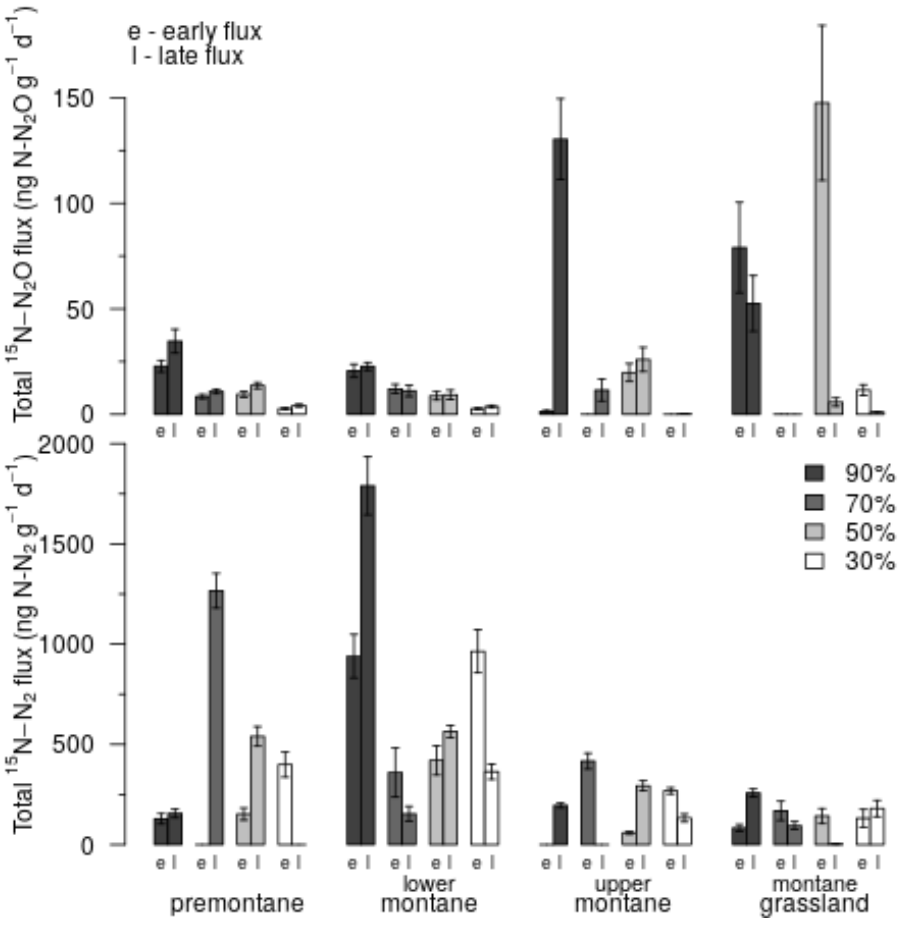

Biogeosciences Discuss., doi:10.5194/bg-2017-107, 2017
Manuscript under review for journal Biogeosciences
Discussion started: 30 March 2017

Figure 5. (a) ^{15}N-N_2O flux and (b) ^{15}N-N_2 flux during the early (≤24 hours) and late (>24 hours) incubation phases of the NO_3^- addition experiment. Results from the +50 % NO_3^- addition are shown in dark-grey, while data from the +100 % and +150 % treatments are shown in mid-grey and light-grey, respectively. The bar charts show means and standard errors.